LAPPEENRANTA UNIVERSITY OF TECHNOLOGY
LUT School of Energy Systems
LUT Mechanical Engineering

*Andreas Uwaoma*

**RECOVERY OF INDIUM FROM LCD SCREENS USING MECHANO-PHYSICAL PRE-TREATMENT**

Examiners: Professor Timo Kärki
D.Sc. Sami Virolainen

## ABSTRACT

Lappeenranta University of Technology
LUT School of Energy Systems
LUT Mechanical Engineering

Andreas Uwaoma

**Recovery of indium from LCD screens using mechano-physical pre-treatment**

Master's thesis

2018

61 pages, 25 figures, 26 tables and 2 appendixes

Examiners: Professor Timo Kärki
D.Sc. Sami Virolainen

Keywords: indium, LCD, pre-treatment, mechanical extraction, leaching.

Recovery of indium from secondary sources such as LCD screens has become important due to the European commission's classification of indium as a critical raw material. Current methods for the recovery have proven unsustainable due to the enormous amount of chemical waste associated with the extraction. In this thesis, we study the separation of the indium-tin-oxide (ITO) layer using different mechano-physical pre-treatments. Four different pre-treatment approaches were applied in the extraction. Heat, plasma, laser, and no pre-treatment prior to mechanical abrasion by a powered brush. The powdered extracts recovered was leached for indium using common mineral acids within technically feasible conditions. Attention was also paid to the economic feasibility of each method against the current market price of indium.

The Indium recovered was concentrated from 0.02 wt.% common in the conventional process to between 7.54 - 15.58 wt.% using the mechano-physical methods. The purity of the indium was up to 93 % and it had a significantly low iron contamination at 0.72%.
Although physical pre-treatment improves the concentration of indium, the cost of the treatments per square-meter of treated of LCD glass makes plain mechanical abrasion a viable alternative.

**ACKNOWLEDGEMENTS**

I would like to thank the examiners of this thesis, Professor Timo Kärki and Post-doctoral researcher Sami Virolainen their unalloyed support in completing this thesis. I also like to thank Post-doctoral researcher Ville Lahtela, Laboratory technologist Toni Väkiparta and the staff the chemical laboratory for their assistance through the most challenging aspects of the thesis.
Finally, thanks to my family for supporting and encouraging me through the endeavors.

Andreas Uwaoma
Lappeenranta 27.09.2018

## TABLE OF CONTENTS

## LIST OF SYMBOLS AND ABBREVIATIONS

ABS: Aqueous biphasic systems

BSE: Back scattered electron emission

CCFL: Cold cathode fluorescent lights

CF: Colour filter

CRM: Critical raw material

D2EHPA: Di-(2-ethylhexyl) phosphoric acid

EDS: Energy dispersive spectroscopy

FE-SEM: Field emission scanning electron microscope

EL: Effective life

EPA: Environmental protection agency

HAZ: Heat affected zone

HEBM: High energy ball milling

ICP-MS: Inductively coupled plasma mass spectrometry

ITO: Indium-tin-oxide

LCD: Liquid crystal display.

mg/L: milligram per litre

mg/kg: milligram per kg

PCB: Printed circuit board

PEG: Polyethylene-glycol

RF/DC: Radio frequency/Direct current

SEM: Scanning electron microscope

TBP: Tributyl phosphate

TFT: Thin film transistor

WEEE: Waste electrical and electronic equipment

# 1 INTRODUCTION

The amount of WEEE (waste electrical and electronic equipment) has increased with technological innovations and social developments. WEEE may contain toxic substances and valuable components which should be separated into its own fraction and from other materials. A certain kind of valuable component is indium that is a critical metal according to classification of European Commission. It is a soft, ductile and malleable silvery metal and it is not found as a natural ore of the earth crust. However, it exists in the ores of other minerals and it can be recovered as a coproduct of their refining process of which the main production occurs in the far east (Setis-MIS, 2016; Minerals yearbook, 2015.) Indium is a group 13 element with atomic number 49 in the periodic table. Pure indium is solid and has a density of 7.31 g $cm^3$ at room temperature. The thermal properties are; melting point of 156.60 ºC, boiling point 2027 ºC and specific heat capacity of 233 (J $kg^{-1}$ $K^{-1}$) (Periodic table-indium, 2017.)

The main source of indium is zinc-sulphide mineral ore (sphalerite) and the indium content of this ore is less than 1 - 100 mg/kg. The low concentration in the mineral ore, low impact of its production on revenue and lack of interest are often affecting production and the quantity available worldwide. (Setis-MIS, 2016; Minerals yearbook, 2015). Indium together with tin-oxide in form of indium-tin-oxide (ITO) is mainly used in the production of transparent conductive films and coatings of flat panel displays – liquid crystal displays (LCD) glass. A large amount of this is often disposed at the end-of-life of the equipment.

## 1.1 Sources and utilization of indium

According to the information on the European commission website, the total world estimated production of primary refined indium in 2013 was 770 tons, out of which 81% originates from the Far-east namely China, South-Korea and Japan with 53%, 19% and 9% respectively. While the consumption data shows that 56% of the application of the refined material was used in the manufacture of flat panel displays (Setis-MIS, 2016.). Secondary refined indium production capacity was estimated as 610 tons for the same year (Lokanc et al, 2015), a bulk of this comes from the recycling of LCD manufacturing wastes, rather than end-of-life product recycling. Figure 1 shows area of application of world indium consumed in 2010.

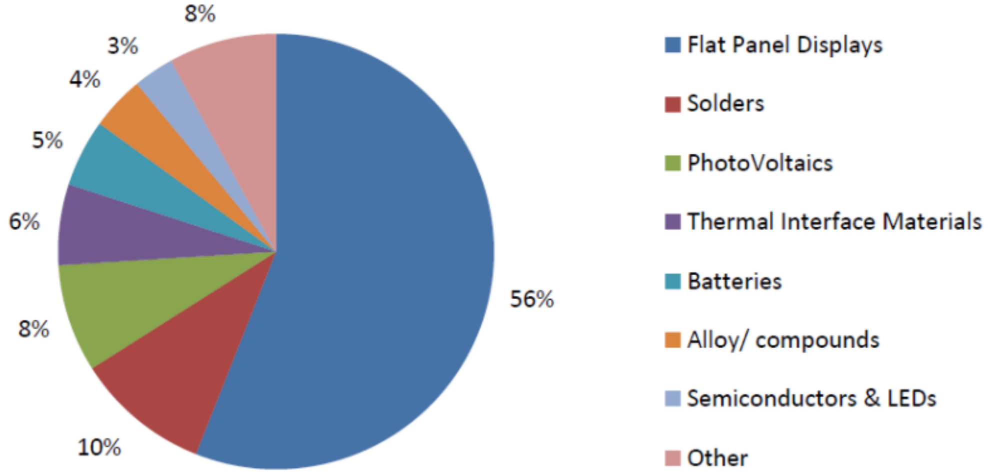


**Figure 1.** Consumption of world indium, 2010. (Setis -MIS,2016)

The pure indium consumed mainly comes from zinc refining, but due to the enormous portion of indium consumed in the manufacture of flat panel display screens, the recycling of end-of-life LCD is becoming a compelling source of indium for the markets.

## 1.2 Importance of indium

Indium has been classified as a critical raw material (CRM) according to the European commission. It is a vital raw material used in the production of broad range of products for which reliable and unhindered access is a concern. Availability of such CRMs may change quickly because of trade flows or changes in policies thus the underlying need for alternative sources to be explored. In the reviewed list of CRMs 2017, the main global producers were identified as China, South Korea and Japan. The sources of EU supply for the years 2010 – 2014 were China - 28%, Belgium - 19%, Kazakhstan - 13%, France - 11%, South Korea - 8% and Hong Kong - 6%. This shows that over 55 percent of the product used in the European Union was sourced from Asia. While end-of-life recycling input rate for same period was 0 % (European Commission – COM, 2017.)

In the USA, imports accounted for all indium consumed between years 2013 -2017. The import sources for the years 2013- 2016 (Minerals information, 2018) shows Canada accounted for 22%, China 22%, France and Republic of Korea both 11% and the rest 33% from other sources. The domestic consumption was 120 tons annually for this period. This high dependence on imports by major consumers makes secondary sources such as end-of-life LCD recovery of indium alternative.

## 1.3 LCD waste stream

Many researchers have attempted in the past to estimate the amount of LCD in WEEE streams. This has proven to be a challenge since state and private run electronics take-back programs from which most data are collected do not track WEEE to the desired degree of detail. To estimate the amount of LCD in the wastes stream, researchers have however relied on material flow analysis, based on the principle of material balance. This quantifies the stock using inflow and outflow of materials of interest through a system in a defined time epoch, where the inflow refers to the total volume of products including imports, and locally produced and outflow represents the total volume of products expected to enter the waste stream. It does not differentiate between products designated for reuse, recycling or directly disposed after the product has reached its obsolescence or after a period of storage with a household.

### 1.3.1 Waste stream Europe and Finland

In the European economic area, an estimation of the quantities and composition of flat screen display devices projected annually for disposal was made using sales figures for LCD monitors, Laptops and LCD TVs, average weight data and the use phase of the device (Salhofer et al., 2011.) For laptops and monitors, the use phase was 4 years and for television 10 years. It was projected that 231000 tons of electronic waste comprising mainly of laptops and monitors will reach end-of-life stage per annum. While LCD TV's will begin to reach their end of life use after 2012. Figure 2 shows an estimation of the mass of end-of-life appliance with LCD screens in 1000 tons.

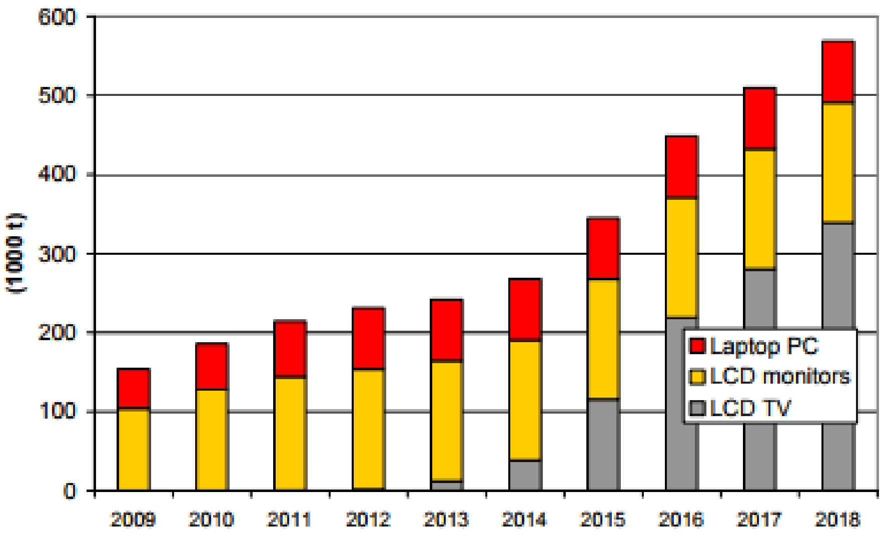


**Figure 2.** Estimation of mass of end-of-life appliances with LCD screens EU (in 1000 tons) (Salhofer et al. 2011).

LCD TV begins to appear in waste stream in 2013, prior to this, mainly computer monitors, and laptop screens are present. Currently, smaller appliances such as tablet and smartphones not accounted for in this estimate will be part of the waste stream though they were not as common before 2009 (Salhofer et al., 2011.) The size of flat panel displays is given by the length of the diagonal in inches and aspect ratio. The most common aspect ratio for both TV and monitor is nowadays 16:9, while sizes start from as low as 14 inches for monitors to 40 inches and TV sizes ranges from 28 inches to up to 70 inches. (NEC display, 2001.)

A more detailed data of LCD waste amount by mass obtained from waste recycling Kuusakoski Oy Finland (Savolainen J., 2017), estimates the amount of waste LCD panel in Finland and European Union between years 2014 and 2022, as shown in Table 1. However, the origin of the data was not specified in the correspondence. The weight of the glass is reported to be 50% of the actual LCD panel.

*Table 1. LCD panel waste amount by mass in Finland and European union (adapted from Savolainen J.,* 2017*)*

| Area | Year | Total SDA + ITC WEEE (tons) | LCD (tons) | LCD panel (tons) | LCD panel weight after plastic removal (50%) (tons) |
|---|---|---|---|---|---|
| Finland | 2014 | 35,000 | 1,750 | 175 | 88 |
| Finland | 2018 | 38,500 | 3,850 | 385 | 193 |
| Finland | 2022 | 42,350 | 12,705 | 1,271 | 635 |
| EU | 2014 | 4,060,000 | 203,000 | 20,300 | 10,150 |
| EU | 2018 | 4,466,000 | 446,600 | 44,660 | 22,330 |
| EU | 2022 | 4,912,600 | 1,473,780 | 147,378 | 73,689 |

### 1.3.2 Waste stream USA

A study by the sustainability consortium (Mars et al, 2016), by Arizona state university published in the report “the electronic recycling landscape, 2016” estimates that American households have 470 million units of small e-waste items and 277 million units of large e-waste items both in use and stored for disposal. Of this amount, smartphones and flat estimating flat panel display recycling turnover as most owners tend to hold dysfunctional electronic items in storage several years above the estimated lifespan (ibid.). There is no exact information on the volume of TFT - LCD devices disposed in the U.S annually as most data consist of TFT-LCD devices and other peripherals. The TFT-LCD devices include flat screen television, desktop computer monitors or laptop screens. So, a rough estimate of expected TFT-LCD in waste streams can be made from shipments data and the average lifespan of these devices. Figure 3. shows a forecast of TFT-LCD TV shipments to the US as at 2013. The number of units was projected at to grow from 37.8 million to 39 million in 2017 (IHS iSuppli Research, 2013).


**Figure 3.** US TV shipment projections 2013 (*IHS iSuppli Research*, 2013).

Although major manufacturers of TFT-LCD devices claim that the product is designed to run for 60,000 hours under controlled conditions at 25 ºC. A study by environmental protection agency (EPA) estimated the average lifetime of TFT-LCD devices to 45, 000 hours, with a primary usage time of 4 years and secondary usage time of 2.5 years before disposal. This was estimated based on the effective life (EL) of the product, i.e. the number of average hours the product is used in the high power and low power mode per annum. Although as display technology turn-over is rapid, these devices are often replaced before the estimated effective lifespan. It can be assumed that TFT-LCD devices shipped to the USA are replaced after a 6.5 year [9]. Yearly, it is expected that a large percentage of this is fed to the recycling waste stream through an electronic take-back scheme in cooperation between retailers and manufacturers. An example of one such take-back scheme is LG recycling program. In the past 5 years, starting from 2012, LG electronics in the US recorded an average of 20280 tons (44707973 lbs) of electronic devices, which were mainly TV's, laptop computers, desktop monitors, small screened mobile devices, VCR's and other peripherals (LG recycling program, 2017). Similar programs are run by other electronic device manufacturers (Dell and Sharp) in the USA but no data on volume and class product recycled is provided.

## 1.4 Flat panel displays – LCD structure

The structure of an LCD display is shown in Figure 4. The LCD consists of liquid crystals, a non-hazardous material which is a blend of up to 20 different organic compounds consisting mainly carbon (C), hydrogen (H), nitrogen (N), oxygen (O) and fluorine (F) sandwiched between two ITO glass substrates with the inside surface coated with a thin polyamide layer. (Matharu A.S., 2012; He, Y., et al, 2014.). The TFT-LCD glass substrate is a low thermal expansion coefficient and low alkaline glass material. Polymeric polarizing films are attached to the glass outer surface and colour filters (CF) are embedded in the inner surface of top glass substrate. (He, Y., et al, 2014.)

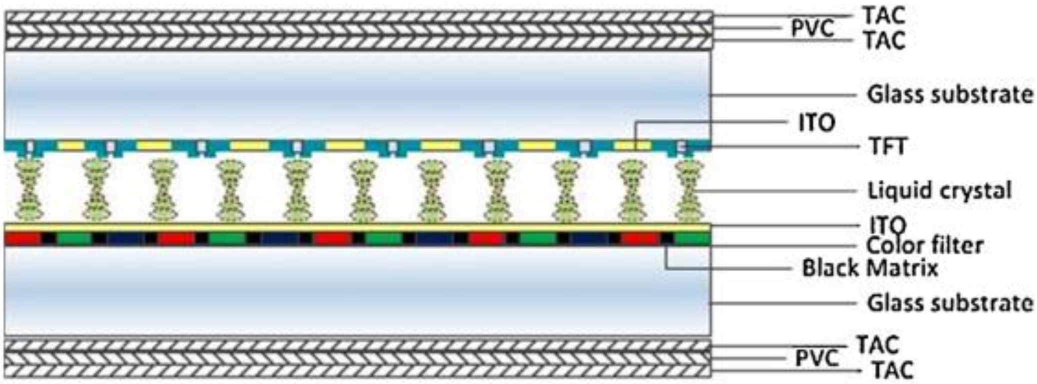


**Figure 4.** Cross-section of TFT- LCD Panel. (He, Y., et al, 2014)

The CF substrate consists of a black matrix, colour pixels, an overcoat layer and ITO film coated atop. The colour filter made from different dye classes is printed on the glass with a black matrix pattern through a photochemical etching process. The TFT glass substrate includes ITO electrodes made on multiple layers heavily doped n-type amorphous silicon followed by Chromium or Aluminium (He, Y., et al, 2014.). This structure is common to electronic devices having LCD in it.

## 1.5 Issues and goals

The aim of this study is to explore mechanical methods for recovery of ITO from the surface of LCD glass before a chemical separation process. Studies on the recovery of indium from waste LCD screens have been performed in the laboratory of Chemical Separation Processes. The LCD glass was crushed with a hammer mill and the material was treated chemically (leaching, extracting). However, the indium content varied between 100-400 mg/kg in the crushed glass, hence, the method is not economical. Preliminary tests relating to the recovery of indium with mechanical machining (ceramic scraper) as a pre-treatment were made by the laboratory of Chemical Separation Processes, and the results of tests have been promising.

In this thesis, the goal is to determine how indium can be recovered from LCD screen industrially such that the process is efficient and economical. The following studies are performed;

- Approaches to recycling of LCD displays.
- Methods and material recovery of indium, with a focus on mechanical treatment as a pre-treatment.
- Tests with selected methods and further processing of indium in the laboratory of Chemical Separation Processes
- Establishing the possibility of adaptation to the recycling of other sandwiched, difficult to recycle materials.

Through the studies, the following questions related to recovery of indium are addressed;

1. What are the possible mechanical methods for improving indium concentration and recovery in LCD glass recycling?
2. What are the design requirements for the possible mechanical methods?
3. How can the mechanical processing methods be practicably implemented on an industrial scale?

By answering these questions, this study tends to find ways to utilize mechanical processing for improving the effectiveness of indium recovery from waste LCD displays, thus providing useful information on the methods, quality and quantity of the indium recoverable from the treatment, and an economic perspective for an industrial scale recycling scheme.

# 2 INDIUM RECOVERY FROM DISPOSED LCD

Pre-treatments are an essential step for material recovery from waste LCD. The first step of the pre-treatment is disassembly of the product. This step is necessary for separation of the LCD screen from plastic housing, cablings, PCB's, and metal parts. It is even more essential as some old LCD display contains Cold Cathode Fluorescent Lights (CCFL) in place of light emitting diodes. It is necessary to safely dispose of CCFL as the leakage of mercury poses a health hazard and harm to the environment (Zhang K, et al 2015.). The disassembly method can be categorized into manual and mechanical disassembly. In terms of value of recovered components and the cost effectiveness of the process, manual disassembly has proven beneficial in comparison with mechanical disassembly (Kopacek B, 2010). Processes such as laser cutting, water-jet cutting, circular sawing would require further research to determine how it could be made economical for industrial use.

## 2.1 Expected quantity of indium from LCD waste

The indium content in LCD glass panels is typically 200–261 mg/kg (Ma et al., 2013; Yang et al., 2013; Lee at al., 2013), although some screens may contain lower amounts of indium 50 -130 mg/kg (Rocchetti et al., 2015; Wang, 2009) or higher amounts 380–410 mg/kg of indium (Hasegawa et al., 2013) and 615 mg/kg (Silveira M.V. et al 2015). The variation in the indium content of LCD's results from the heterogeneity the materials in the cases where the material is sourced from waste stream, the handling can also affect the indium content. Assuming 250 mg/kg of indium can be recovered from LCD glass substrates coming into the waste stream in Finland and Europe, we can estimate the net value of indium in the waste stream as shown in Table 2. In summer of 2017 price of indium $300/ Kg (Strategic-metals, 2017), Table 2. shows the net value indium.

*Table 2. Net value of indium recoverable from LCD waste stream in Europe. (adapted from. Savolainen J., 2017)*

| Area | Year | LCD panel tons | LCD panel weight post-plastic removal (50%) tons | Indium Kg | Net value ($) |
|---|---|---|---|---|---|
| Finland | 2018 | 385 | 193 | 48.25 | 14,550.00 |
| Finland | 2022 | 1,271 | 635 | 158.75 | 47,625.00 |
| EU | 2018 | 44,660 | 22,330 | 5582.50 | 1,674,675.00 |
| EU | 2022 | 147,378 | 73,689 | 18422.25 | 5,526,675.00 |

## 2.2 LCD glass properties

The CF and TFT substrate in LCD are made from clear non-alkali glass and the standard thicknesses are 0.5 mm, 0.7 mm, and 1.1 mm. The ITO layer is applied on top of a colour filter layer in TFT-LCD while in the LCD it is applied over a silicon dioxide passivation layer with thickness approximately 25nm. Various methods are used in deposition of indium-tin-oxide on a substrate. These include RF/DC magnetron sputtering in vacuum conditions, Ion implantation, ion-beam assisted deposition, such as electron beam evaporation. Some of these are performed at elevated temperatures (Ghorannevis Z, et al. 2015). The thickness of the ITO on substrate can be as low as 150-300 nm depending on the level of transmissivity or conductivity desired. The chemical and mechanical properties of the substrate from AvanStrate, a major manufacturer of LCD glass is summarized in Table 3.

*Table 3. Chemical composition and mechanical properties of LCD - ITO glass. (adapted from: AvanStrate Inc. 2017; glass properties. 2017)*

| **LCD glass substrate** | | | | | | | **ITO layer** | |
|---|---|---|---|---|---|---|---|---|
| $SiO_2$ | $Na_2O$ | SrO | $K_2O$ | BaO | $Al_2O_3$ | others | $In_2O_3$ | $SnO_2$ |
| 71.93 | 8.66 | 6.23 | 5.63 | 4.23 | 1.42 | ~ 7.53 | 90.0 | 10.0 |
| Thickness | | | 0.5, 0.6, 0.63, 0.7 mm | | | | 150 – 300 nm | |
| Density g/cm$^3$ | | | 2.41 | | | | 7.14 | |
| Young’s modulus GPa | | | 73.9 | | | | - | |
| Modulus of rigidity GPa | | | 29.9 | | | | - | |
| Thermal strain point ºC | | | 661 | | | | - | |
| Deformation point ºC | | | 786 | | | | - | |
| CTE: X 10$^{-7}$/ ºC, 50-300 ºC | | | 34.5 | | | | - | |

## 2.3 Physical recovery methods

Several methods have been studied for recovery indium from waste LCD. Most of these methods involves a preliminary mechanical process to reduce the LCD glass into manageable fractions followed by chemical methods for the extraction of the target material. Available literature suggests a combination of comminution and hydrometallurgy as the most established process used in recovery of indium from discarded LCD screens. In the recent, variants to hydrometallurgical extraction or leaching of indium from pulverized ITO glass substrate are being researched and some publications have been made about these methods. This section explores available literature from researchers on indium recovery to clarify key findings.

### 2.3.1 Comminution of LCD substrate

Comminution methods have been studied as a pre-treatment for LCD panels prior to hydrometallurgical extraction. This includes knife milling, ball milling and hammer milling. (Rocchetti et al. 2015; Virolainen et al. 2011). Typically, the LCD panel is crushed into micro sized particles. (Lee, Jeong et al. 2013), investigated the effect of milling time, particle size and leaching time on the amount of dissolved indium recoverable by high energy ball milling (HEBM) of ITO glass. While (Silveira et al., 2015) studied the effect temperature, solid/liquid ratio, concentration of the acid and time on indium recovered. Overall, only about 86% of indium in the ITO glass was recovered. This study showed that at milling time higher than 1 minute, the amount of indium recoverable from the substrate decreases. This was attributed to decrease in surface area of the valuable components due to agglomeration of particles.

Three types of mills were tested for mechanical comminution after dismantling the LCD panel (Ferella F. et al, 2016). The cutting mill was run in three tests, without a sieve, with a 10 mm and 6 mm sieve. A blade mill was run for 10 minutes in two tests with a 10mm and 6mm sieve. While a rod mill was used in 4 different tests of 10, 20- and 30-minutes wet milling and a 20-minutes dry milling. Overall rod milling (wet process) lasting 30 minutes produced the smallest particle sizes of - 212 micrometres and the best separation of glass from plastic. In the hydrometallurgical treatment the wet process also produced better results, 40% of the total LCD weight was recovered as indium containing concentrate, while 20% and 15 % were glass and plastic respectively. The indium recovered in the wet process was 87% like the result obtained by (Silveira et al. 2015), and with 74% in the dry process. Plastic recovery was also 10 percent greater than in the dry process. The concentration of indium in the glass powder was 575 mg/L vs 334 mg/Kg in the dry process.

Attrition scrubbing was examined as a method for concentrating indium from shredded LCD displays to a level that makes hydrometallurgical recovery viable (Boundy et al., 2017). Compared with conventional shredding methods, attrition was shown capable of producing a concentrate with indium content increased by a factor of 10 with above 90% of the indium recoverable.

2.3.2 Mechanical scrapping of glass surface

A mechanical stripping process was investigated as a pre-treatment for ITO glass prior to liquid crystal decomposition by a pyrolysis process and indium recovery (Zhang L., et al. 2017).

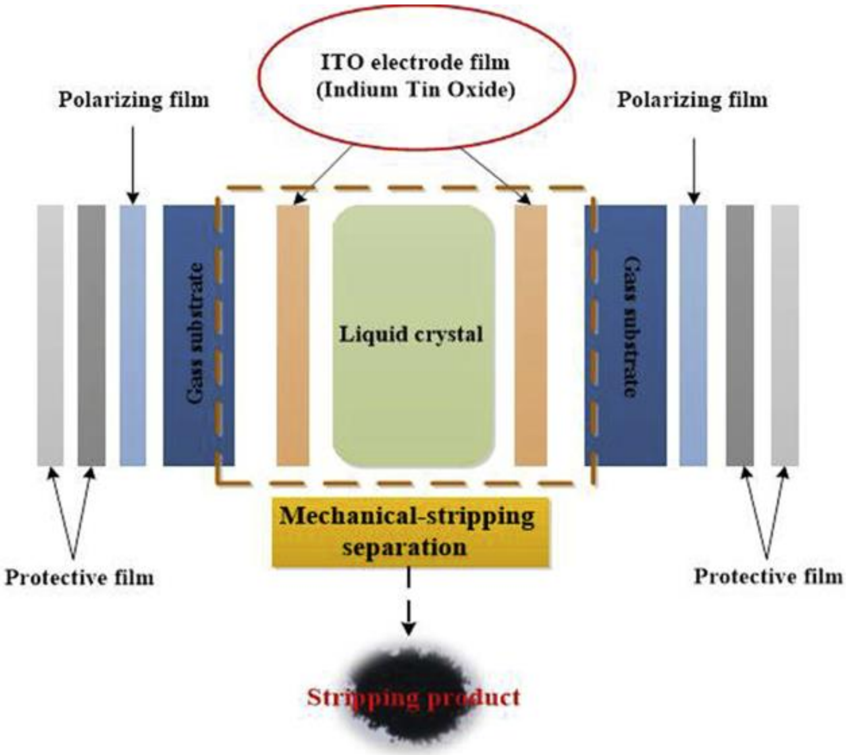


**Figure 5.** Structure of LCD panel and preparation of stripping product.(Zhang L. et al. 2017).

The stripping process involved washing, drying, separation, scraping and grinding of glass substrates with roller brushes. Two pieces of glass substrates were separated, and then the liquid crystals, ITO and a small amount of glass were scraped of the conducting surface using roller brushes. The bounding box in Figure 5 shows the scrapped and ground cross-section of the LCD panel. The stripping product was treated by pyrolytic decomposition. Oil, gas and an indium rich residue was recovered from the process. The residue showed an enriched indium content of 7.95 wt.% from 0.02 wt.% in the glass before the pyrolysis process. A precursor to this research (T. Huhtanen, 2017) has investigated the scrapping of ITO film using a ceramic scraper as a pre-treatment with promising results.

Mechanical exfoliation was also applied for the enrichment of ITO. (Wang S. et al, 2017). In the study “Recovery of valuable components from waste LCD panels through a dry physical method” a dry physical polisher was utilized in abrading the ITO layer on CF and TFT glass. The LCD glass held firmly to the operating platform by applying a negative pressure on the polarizer side of the glass, while the ITO layer was upward facing a polisher made of Al2O3 particles smaller than 400 mesh. The head of the polisher is brought in contact with the ITO layer and as it rotates, it abrades the ITO layer. The ITO concentrate removed is collected into a dust bag through a negative pressure system coupled with the polishing head. Figure 6 shows schematic of the negative pressure polisher configuration.

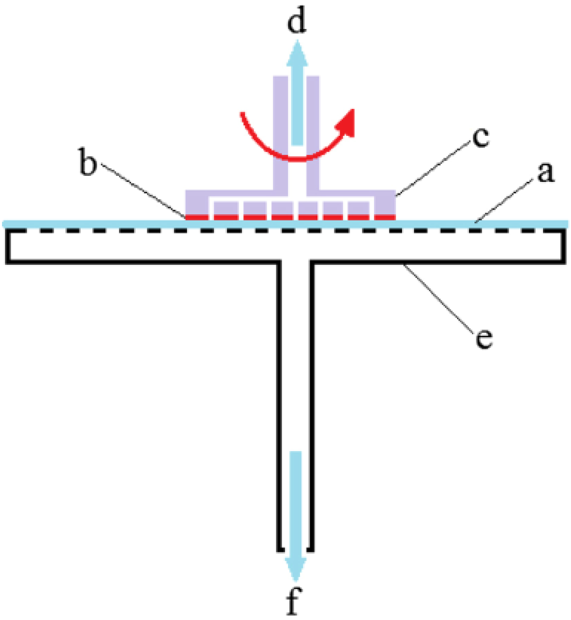


**Figure 6.** Negative pressure polishing scheme. (a) LCD-TFT glass, (b) polishing abrasive (c) polishing head (d) Dust recovery system (e) operating platform (f) working holding negative pressure. (Wang S. et al, 2017.)

The characteristics of the ITO concentrate extracted by dry polishing were analysed and results showed the indium content of the recovered concentrate from CF glass was 7.26 wt.%, a 154-times increase in concentration compared with 0.047 wt.% obtained from original CF glass.  For the TFT glass, recovered concentrate was 4.78 wt.%, compared with 0.032 wt.% in the original TFT glass. The residual CF and TFT glass after the dry polishing process had 0.0020 wt.% and 0.0014 wt.% of indium respectively (Wang S. et al, 2017.). The tin content in the recovered concentrate also showed a similar increase in values for both CF and TFT glass. An important feature of the result is difference in the yield for CF and TFT glass. Indium recovered from CF glass is 1.5 time more than that from TFT glass. This information is useful for estimating the expected quantity of recoverable indium from a given mass of selected LCD waste.

2.3.3 Thermal process

According to He et al. (2014), vacuum carbon reduction can be utilized for recovery of indium from LCD wastes. Preliminary test carried out on pure indium oxide (In2O3) showed the effect of temperature and vacuum carbon process was reduction of indium oxide to metallic indium. LCD glass was crushed to powder and sieved to sizes smaller than 0.3mm. Coke powder with over 80% carbon content and sizes 0.8mm was used as a reducing agent. The LCD powder was mixed with carbon at selected mass ratios and treated at temperatures 1073,1123, 1173, 1223 and 1273 K. Indium evaporated into gas phase and was collected by condensation at a low temperature zone. The recovery rate of indium peaked and remained steady at temperatures above 1173 K with 100% pure indium was recovered. The best parameters for reclamation were confirmed at 1223 K at vacuum pressure of 1 Pa with 30 wt.% of added carbon(coke) in 30 minutes. The effect of the reduction process on the tin-oxide content of ITO was examined. SnO2 in the panel was decreased from 196 mg/L to 110 mg/L. However, this did not lead to the impurity Sn in the recovered indium since the vapor pressure of Sn (0.002 Pa) differs significantly from the optimal 1 Pa for indium. An analysis of the recovered material indicated that 90 % indium could be recovered at the obtained parameters of 1223 K, 1 Pa with 30 wt.% of reductants.

## 2.4 Hydrometallurgical process

Hydrometallurgy, a process for extraction of a metal from its ore by dissolution into an aqueous solution of a salt of the metal and recovering the metal from the solution by method of solvent extraction is also an established method for recovery of indium from waste material. The hydrometallurgical process as applied in indium recovery is performed in two steps. The first is leaching and dissolution of the indium rich material into a solution using mineral acids followed by solvent extraction of metals from the resulting solution using extractants.

### 2.4.1 Leaching and dissolution

The leaching kinetics of indium, tin, iron and aluminium was studied (Jiaxu Y, et al. 2012) using 0.1 M, 1 M and 6 M concentrations of nitric acid ($HNO_3$), sulphuric acid ($H_2SO_4$) and hydrochloric acid (HCL) on shredded LCD glass without removal of polarizer film. In recovery of indium from indium tin oxide by solvent extraction (Virolainen et al 2011 a) utilized acid concentrations of 0.001, 0.01, 0.1 and 1 Mol. in leaching experiments performed on ITO nano powder. The study showed the selectivity of dissolution of indium and tin at different concentrations of the acidic media as means of selectively recovering aqueous salt of the metals.

In both studies, the substrate is mixed with the acid and mechanically stirred to aid the dissolution. Two substrates to acid mixes was used. 1 Mol. sulphuric acid ($H_2SO_4$) solid to liquid ratio 10:1 (Virolainen et al. 2011 b, Jiaxu Y, et 2012) and 3:1. The leachate is collected at time periods ranging from a few minutes to hours. Metal concentration in the leachate is determined using inductively coupled plasma mass spectroscopy (ICP-MS) and quantified against a set standard (Virolainen et al 2011; Jiaxu et al 2012.).

### 2.4.2 Solvent extraction

Separation of the metals indium and tin from the leachate are performed using known extractants. 1 Mol. Di-(2-ethylhexyl) phosphoric acid (D2EHPA), 1 Mol. tributyl phosphate (TBP) and a mixture of 0.2 Mol. D2EHPA + 0.8 Mol. TBP. Both metals are extracted from $H_2SO_4$ solution with D2EHPA followed by selective stripping of indium using HCL of concentrations higher than 1.5 Mol. (Virolainen et al. 2011 b.) An alternative approach is selective extraction of Tin using 1.5 Mol. HCL. DEHPA diluted in kerosene is also suitable for selective extraction according to (Jiaxu et al. 2012). 0.1 Mol. -1 Mol. $H_2SO_4$ is used for extraction while 1 Mol. HCL is used for stripping. The calculations on extraction from 0.1 M $H_2SO_4$ showed that indium could be recovered from leach liquor and separated from other impurities.

Indium can also be extracted with Polyethylene-glycol (PEG) based aqueous biphasic systems (ABSs) consisting of Polyethylene-glycol, ammonium sulphate and water (PEG-$(NH_4)_2SO_4$-$H_2O$). (Fontana et al. 2015) Two phase solvent extraction yield for indium were 110 mg/L bottom phase and 17 mg/L phase this offers a better yield compared with results 76.16 mg/L of indium and 10.24 mg/L tin obtained by (Swain et al, 2016) using 5 M hydrochloric acid, at temperature 75 ºC, hydrogen peroxide of 10 v/v% and 500 g/L pulp density.

### 2.4.3 Ultrasonic assisted leaching

New process pathways are being researched for higher yields of the recovered material. A non-crushing leaching with the aid of an ultrasonic wave, (K. Zhang et al. 2017) was proposed as a method of extracting indium from ITO glass without the need for comminution of ITO glass substrate. The glass is immersed in acid solution with the ITO film side only in contact with the acid. An ultrasonic wave is used to induces acoustic cavitation i.e. bubble formation and growth on the ITO film surface. When the bubble collapses, high pressure shock waves and micro jets are generated at the interface resulting in a gradual surface erosion and a solid/liquid mass transfer (Souada et al. 2018) also investigated ultrasonic assisted leaching for indium and tin from ITO glass surface. The rate of dissolution as a function of leaching time was studied in the presence and absence of ultrasonic activation, using concentrated sulphuric acid (18 mol./L) at 60 °C. The result shows the ultrasonic activated procedure reaching a steady state at 4 minutes, where 82% of indium was dissolved in comparison with 13% in the absence of ultrasonic activation. The total indium recovered was above 92% in the presence of ultrasonic activation and about 70% in absence. This method offered a simplified process for recovery of indium while the glass resulting from the ultrasonic activated process could be recycled without additional separation processes (Souada et al. 2018.) One thing that was noticed during literature search was an absence of unified quantification or measure of recovered material. Some researchers reported in terms of wt.% of ITO glass while others reported in terms of amount leachate to glass ratio.

### 2.4.4 Sub critical water treatment

Indium was successfully extracted from CF glass using subcritical water. According to (Yoshida, H., et al 2014) treatment of LCD wastes at different temperatures and reaction times resulted an average recovery of 83% of indium from CF glass and 7% from TFT glass at 360 ºC. In the experiment, the LCD panel was stripped, separated and cleaned to remove the liquid crystals material. Thereafter substrates were cut to the sizes of 5-10 mm and treated in a batch reactor with pure water at subcritical temperature. After treatment, the specimen was cooled, and solid residues were separated from an aqueous phase by vacuum filtration. The amount of indium recovered from the medium was compared with that of fresh LCD by material balance. The result of the study indicates that treatment with subcritical water at temperature 360 ºC is a suitable approach for recovery of indium from CF-glass. The glass material leftover is also clean and suitable for reuse for new LCD substrate since there are no changes to the glass chemical properties.

## 2.5 Comparison of recovery methods

Comparing the different processes based on the concentration of indium in recovered material, the mechanical stripping process offers an advantage as a pre-treatment method Indium content of the stripped material was 7.95 wt.%, an increase compared with 0.02 wt.% obtainable from comminution of entire LCD glass substrate. A summary of literature findings is presented in Table 4.

*Table 4. Summary of results from literature.*

| **Methods** | **Post treatment: Leaching and solvent extraction** | | |
|---|---|---|---|
| Comminution | | Recovered % | In. wt.% |
| - HEBM | Required | 86 | 0.011- 0.029 |
| - Rod milling (wet) | Required | 87 | 0.027 |
| - Rod milling (dry) | Required | 74 | < 0.020 |
| Mechanical Stripping | Required | - | 7.95 |
| Thermal - Vacuum carbonization | Condensation | 90 | - |
| Subcritical water process | Filtration & drying | 83 | 0.0337 |
| Ultrasonic process | Required | 96 - 100 | - |

Considering the sustainability of the methods, mechanical stripping also performs better as the amount of material processed chemically post stripping is smaller. In the next chapter, the materials for the experiment, the methods and experiment setup details are discussed.

# 3 MATERIALS AND METHODS

The materials for this experiment LCD panels are supplied by the participating organization, Kuusakoski Recycling Finland. The material includes different sizes of LCD panels, some in good condition without major cracks. The heterogeneity of LCD screen sizes necessitated a sorting phase in preparation for the experiments. The LCD panels were thus inspected and sorted according to the size of the panels. Effort was made to determine LCD panel origin and to ascertain the variations in LCD panels made by the different manufacturers, but this was not successful as discernible identity markings were absent.

## 3.1 Material details

Five different panel sizes were selected for this experiment as shown in Table 4, the smaller panel sizes being the most common. The ITO layer on both CF and TFT substrate estimated as 150nm thick (Thin film products 2017, p. 2). The density grade of target material is >99.5% based on ITO with 90/10 wt.% ratio. If density of the sputtered material is of similar value, ITO density on LCD is 7.14 g/cm$^3$. The theoretical amount of indium (g) in 1000 units of the panel can calculated as shown.

$$\text{Mass (g)} = 0.9 * \text{density (g/cm}^3) * \text{Area (cm}^2) * \text{thickness (cm)} * 2 \tag{1}$$

$$\text{Mass (mg)} = \text{Mass(g)} * 1000$$

Where 2 represents the CF & TFT substrate. Table 5. Shows the theoretical amount of indium in mg/kg for each of the LCD samples based on 150nm thick layer of ITO.

*Table 5: Expected indium amount for 1000 units of TFT and CF substrate.*

| # | Area (cm$^2$) | Weight of LCD (kg) | Indium (mg) / LCD | Est. Indium mg/kg | Total weight of 1000 LCD (kg) |
|---|---|---|---|---|---|
| LCD1 | 489.5 | 0.201 | 94.4 | 469.6 | 200.9 |
| LCD2 | 740.2 | 0.292 | 142.7 | 489.2 | 291.7 |
| LCD3 | 1300.0 | - | 250.6 | - | - |
| LCD4 | 1228.5 | 0.485 | 236.8 | 488.5 | 484.7 |
| LCD5 | 1503.5 | 0.590 | 289.8 | 491.7 | 589.4 |

The actual amount of indium in the LCD according to literature ranges between 200 - 261 kg. However, the theoretical amount calculated is approximately twice this value

## 3.2 Experimental setup details

Four different recovery approaches are to be investigated in the experiments. Mechanical abrasion, heat treatment and mechanical abrasion, plasma treatment and mechanical abrasion, and laser treatment.

### 3.2.1 Equipment

The resources for experiment are as follows:

Brushing – Electric hand tools

- Abrasive roller brush model Makita 9741 using aluminium oxide-based sanding lamella roller K240.
- Hand sanding tool- model B&D duosand KA330E with aluminium oxide based abrasive paper, grit size P60, P80, P100, P150
- Blotter – material recovery, dust recovery vacuum.

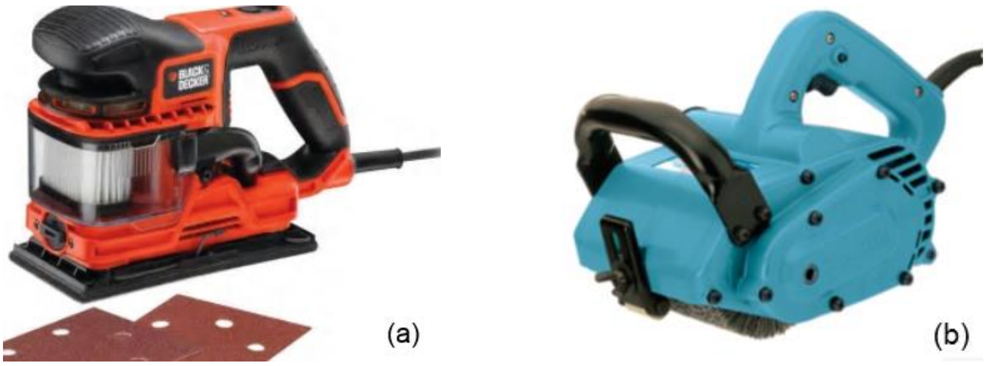


**Figure 7.** Power tools (a) hand sanding tool (b) hand held dry roller brush

The hand-held dry sander shown in Figure 7.a comprises an integrated blotter/vacuum for dust collection while the dry roller brush Figure 7.b requires an external dust collection system.


**Figure 7c.** Sanding roller lamella K240

Laser - Processing device

- 2.5 KW $CO_2$ Laser.
- Working area 1 × 0.5 m.

Plasma - cold plasma device.

- Plasma generator FG 5001
- Plasma head RD 1004

  Power 1 kW, Spin speed > 2000 rpm, plasma processing width >50 mm, scan speed 0.33 m/s for processing width of 40 mm.

  Nozzle offset distance 4 -15 mm.

  Gas: Oil and water free compressed air 2 $m^3$/h, pressure 4-8 bar.

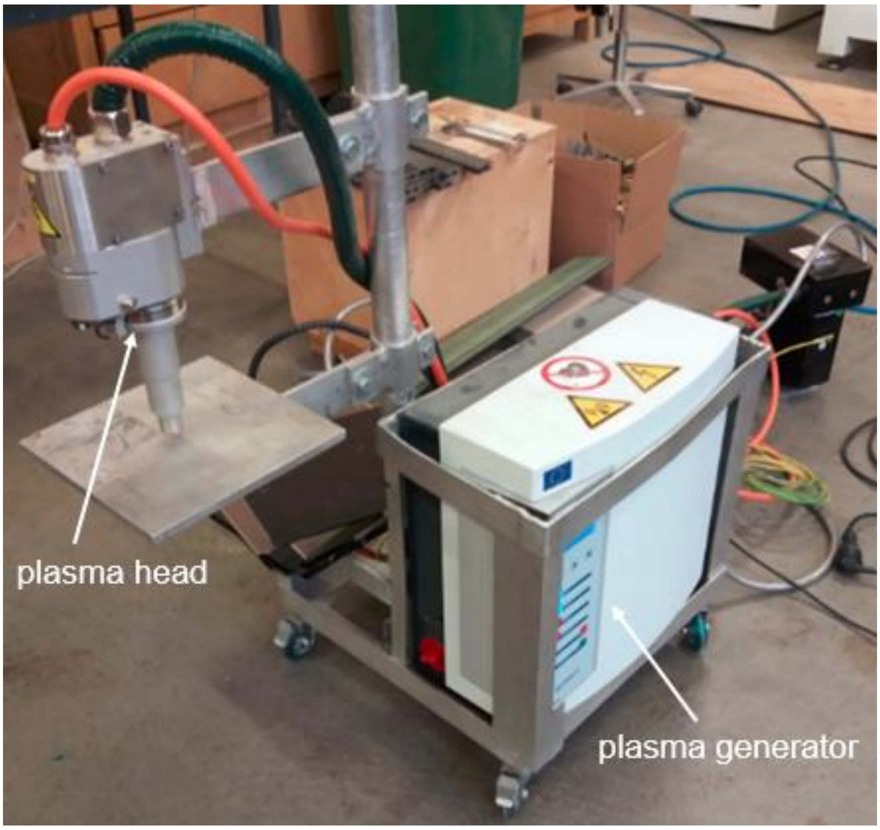


**Figure 8.** Cold plasma device, comprising generator FG5001 and plasma head RD1004.

Heat treatment – Test will be performed in chemical laboratory and Scanning electron microscope (SEM) analysis also provided by the chemical laboratory.

### 3.2.2 Material preparation

Three different approaches are planned for recovery as shown in Figure 9. First the material preparation process. Sorting and selection of the panels to process is performed and the panels are split into CF and TFT substrate by prying between sheets with a thin knife, thus exposing the liquid crystal material. Care is taken to ensure the glass substrate remains attached to the plastic polarizing film during this process. Then liquid crystal is wiped off the conducting film using an acetone laden blotting paper, after which the substrate left to dry. Elementary brushing experiment without pre-treatment is performed for some LCD samples.

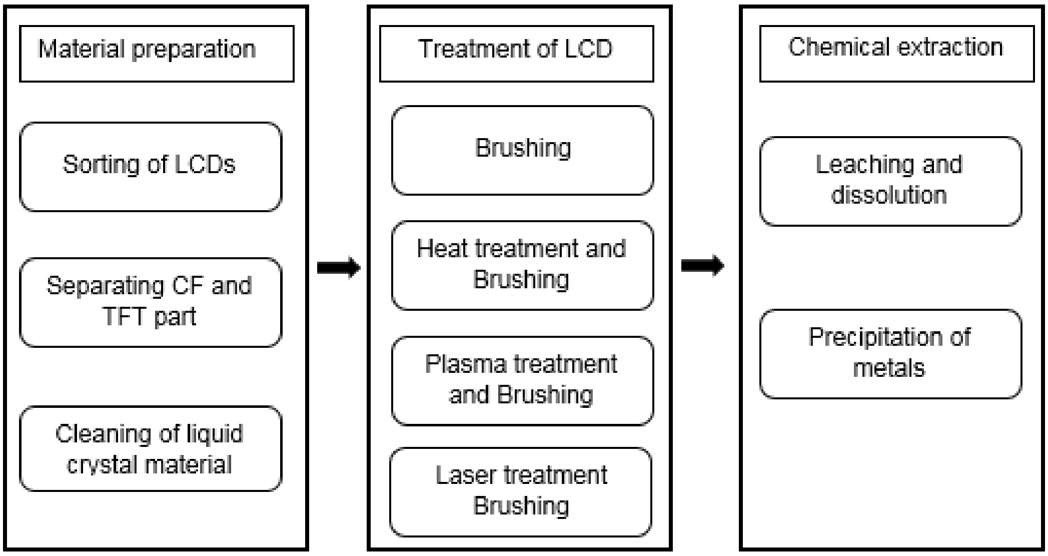


**Figure 9.** Indium recovery process chart.

The treatment methods include Heat treatment + brushing and plasma treatment + brushing and laser treatment. Preliminary experiment will be performed using hand tools – Brushing/roller abrasion setup can be replicated using a powered sander with abrasive paper. A system to collect removed material - a lower power vacuum with appropriate filter and dust collection material will be utilized. Measurements of quantity of material for preliminary experiment will give an idea about abrasion time, and the range of possible abrasive grit sizes.

### 3.2.3 Brushing process

The input (factors) that are important for material recovery by the brushing process are abrasive grit-size (X1) and time (X2). The relative effect of each of the two factors on the yield (Y1-g) of material recovered will be ascertained in the experiment. The grit size is varied stepwise according to grid class while the time is constant in the preliminary experiment. The grit that results in an increased rate of recovery for the specified time is determined. The material removed is collected for further analysis and chemical extraction process. The inputs are described in table 5, factor level settings. Other abrasive grit sizes that will be investigated are P40, P120, P180, P220. The brushing time varies according to the size of the LCD screen and the substrate type. Three different trials were made to determine average brushing time. For LCD 5, with surface area 1053.5 $cm^2$, the minimum brushing time was 60s for CF substrate and 80s for TFT substrate. Average brushing time for LCD5 (CF and TFT substrate) is 70s. The values for the LCD1, LCD2, LCD3 and LCD4 are thus estimated based measured values of surface area.

*Table 5. Factor level settings.*

| | Low (-1) | Mid (0) | High (+1) | Standard/unit |
|---|---|---|---|---|
| Grit | P80 | P60 | P100 | ANSI |
| Time | t1 | t2 | t3 | sec |

*Table 6. $2^2$ Two-level factorial design table in standard order.*

| | Grit-size, X1 | Time, X2 |
|---|---|---|
| 1 | -1 | -1 |
| 2 | +1 | -1 |
| 3 | -1 | +1 |
| 4 | +1 | +1 |

The experiment is ordered as shown in table 6. Including central values. The central value is run at the beginning and at the end of the experiment of the experiment.

*Table 7. Design table and experiment run order.*

| | Grit-size, X1 | Time, X2 |
|---|---|---|
| 1 | P60 | t2 |
| 2 | P80 | t1 |
| 3 | P100 | t1 |
| 4 | P80 | t3 |
| 5 | P100 | t3 |
| 6 | P60 | t2 |

P60 was ineffective using the hand grinder, this was observed through a visual inspection of the CF substrate after grinding for 70s, the dark matter was only partially abraded. Thus, the number of experiments is reduced to avoid replication of parameters and repetition of values that have been found ineffective. Figure 10 shows the brushing process and the surface of the substrate after two passes of brushing.

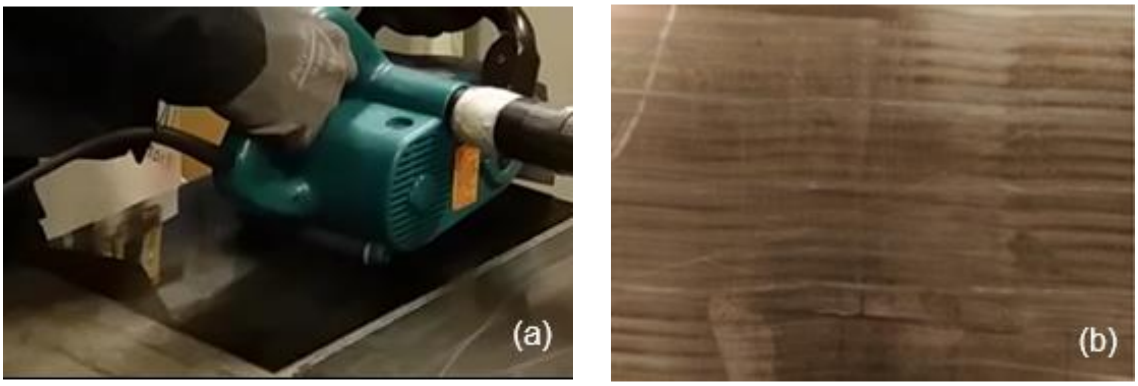


**Figure 10.** LCD substrate (a) brushing process (b) surface post brushing process.

3.2.4 Heat treatment and abrasive brushing process

In the crystallization annealing process in open air that was investigated by (Alkhazaili et al. 2015), replication of SnOx was responsible for the crystal structure obtained in annealing. Thermally reducing the InSnO5 in the absence of oxygen is expected to alter the structure of the ITO layer due to loss of the oxide bonds. The expected result is a transformation of the ITO from a crystalline to the back to a weaker amorphous structure. In this experiment, we investigate how material removal is affected by heat treatment. Heating will be applied as a ramp starting at room temperature (20 - 22 ºC) to target T ºC and held for a fixed time and then the material is then cooled to room temperature. The thermal process however has some challenges. The problem of identifying the conductive surface arises once a high temperature thermal process is applied to the LCD glass since the polarizer material is removed or possibly decomposed by the heat in the process, this must be addressed to fully integrate heat treatment into industrial scale recovery.

The heat treatment will be performed at first prior to the abrasive brushing process, to determine its effect on material removal and the quality of recovered material. Temperature is included as an input factor for the design tables developed in the previous subsection. The input factors are now, abrasive grit-size (X1), time (X2), and Temperature (X). The relative effect of each factor on the yield (Y1) of material recovered will be ascertained in the experiment. The factors that were altered in this experiment are the temperature and abrasive grit size. Only two temperature values were tested, 300 and 600 ºC due to schedule limitation. For all samples tested, the heating time was than 30 minutes. However, the material remained in the oven over four hours in each case as the cooling rate and fume extraction was slower. Moreover, the fragile nature of the material after heating made it unsafe for handling until considerably cooled. The effect of thermal treatment on the recovery and grinding time was observed. Table 8. show input variables (factor levels) for the combined thermal and abrasive process.

Table 8. Factor level settings for combined thermal and abrasive process.

| | Low (-1) | Mid (0) | High (+1) | Standard/units |
|---|---|---|---|---|
| Grit size | P80 | P60 | P100 | P - Grade |
| Time | t1 | t2 | t3 | sec |
| Temp. | T1=300 | T2=0 | T3= 600 | ºC |

The experiment is ordered as shown in Table 9. The central value is run at the beginning, mid-point and at the end of the experiment.

Table 9. Design table and experiment run order

| | Grit-size, X1 | time, X2 | Temp. X3 |
|---|---|---|---|
| 1 | P60, 0 | t2, 0 | *T* 2, 0 |
| 2 | P80, -1 | t1, -1 | *T* 1, -1 |
| 3 | P100, +1 | t1, -1 | *T* 1, -1 |
| 4 | P80, -1 | t3, +1 | *T* 1, -1 |
| 5 | P100, +1 | t3, +1 | *T* 1, -1 |
| 6 | P60, 0 | t2, 0 | *T* 2, 0 |
| 7 | P60, 0 | t2, 0 | *T* 1, -1 |
| 8 | P80, -1 | t3, +1 | *T* 3, +1 |
| 9 | P100, +1 | t1, -1 | *T* 1, -1 |
| 10 | P100, +1 | t1, +1 | *T* 3, +1 |
| 11 | P60, 0 | t2, 0 | *T* 2, 0 |

### 3.2.5 Plasma treatment and brushing

Atmospheric plasma surface pre-treatment is widely applied in removing organic contaminants and enhancing the adhesion of coatings on materials such as plastics, metals, and composites. Plasma surface modification can also be used to create patterns on a surface. The process is referred to as etching and it is used in the production of printed circuit boards. Plasma is created when gas in a chamber is ionized by an electric charge thus creating ions. These ions when impinged on a material surface react with the outer layer of the material modifying it on a molecular level. Chen et al. (2017) Investigated the effect of plasma treatment time of surface characteristics of ITO films. It was established that O2-Plasma treatment altered the grain structure of the ITO film. The grain structure of the ITO film became less obvious with increased treatment time. Figure 11. Field emission Scanning Electron Microscope (FE-SEM) images compares the surface roughness of treated and untreated ITO.

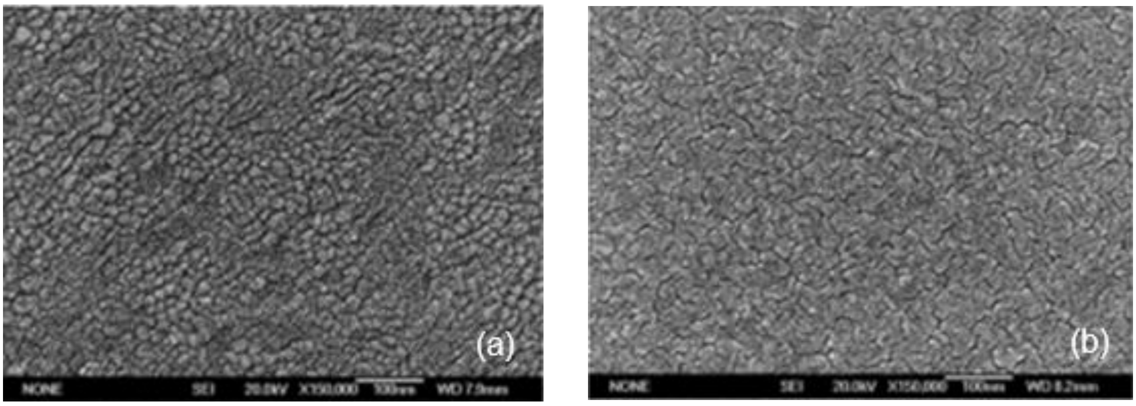


**Figure 11.** FE-SEM images representing surface roughness of (a) pure ITO and (b) $O_2$-plasma treated bulk ITO 180 seconds.

Similar changes in grain structure was observed for ITO treated for 300 seconds. The mean surface roughness value for treated ITO was $R_{rms}$: 0.821 and 0.805 nm for 180s and 300 seconds exposure respectively, compared with a $R_{rms}$: 0.864 nm which is larger for untreated ITO (Chen et al, 2017.). In our plasma treatment experiment, the influence of cold atmospheric plasma on the structure of the ITO prior to brushing is studied and the effect of the treatment on the recovered material will be analysed. TFT and CF substrates were exposed to atmospheric plasma through a rotating nozzle for 1, 2, and 5 seconds respectively. Figure 11 shows the plasma treatment process and the state of the substrate post treatment.

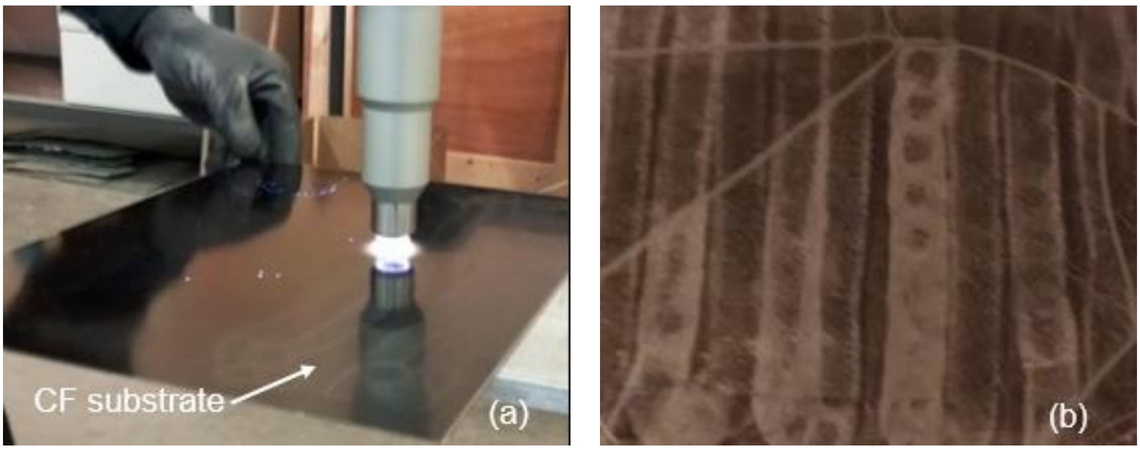


**Figure 12.** Cold plasma (a) treatment process (b) treated CF substrate.

The substrate was manually manipulated under the beam to expose the entire surface area. To ensure complete exposure, a beam overlap of approximately one-fourth nozzle diameter was maintained through the process. On visual inspection, the treated substrates showed colour changes in the areas of exposure, the level of discoloration was also influenced by exposure time.

### 3.2.6 Laser treatment and brushing process

In the fourth approach, laser ablation will be performed on the specimen prior to brushing. A pulsed laser beam will be focused on the material interfacial layers for ITO-CF-Glass split/delamination. The type of laser available for use is undetermined at this point. Typically, CO2 lasers with its wavelength above 10.6 micrometres are suitable for glass materials. Lasers with a higher wavelength simply pass through clear glass and affect the underlying material. The laser beam can produce localized heating on the ITO layer thus affecting the glass ITO interface. The laser treatment trial will include a preliminary experiment to determine the effect of the laser beam on the ITO layer. The experiment can be performed using a pulse modulated wave, this is ideal since at lower average powers less heat is transmitted into the bulk glass at every pulse. The heat affected zone (HAZ) is better controlled with shorter pulses and can be limited to the surface to as low as 0.1 mm. A continuous wave can be utilized at high speeds to ensure low interaction times. Table 10 shows the parameters in laser processing. The laser beam focal position can also be adjusted to be outside or accurately at the ITO layer, but this is depending on the equipment capabilities.

*Table 10. Preliminary laser processing parameters.*

| Reference | Av. pow (W) | Speed (mm/s) | Focal length |
|---|---|---|---|
| I | 200 | 300 | +30 |
| II | 200 | 400 | +30 |
| III | 200 | 500 | +30 |

Three different treatment comprising two specimens per treatment and an untreated/ reference material is studied in the preliminary test. The weight of the samples and geometrical properties are also recorded for further evaluation.

In the experiment laser treatment was unsuitable for the TFT substrate due high reflectivity of the ITO coating. SEM analysis of the laser pre-treated specimens will give information about the state of ITO layer, with this we can ascertain prior to brushing if laser treatment impacts the recovery of ITO. Table 11. Shows the pre-treated specimen values.

*Table 11. Laser pre-treatment specimen for CF substrate.*

| Treatment | No. | weight (g) | Thickness (mm) |
|---|---|---|---|
| Untreated | 1 | 2.15 | 0.939 |
| Untreated | 2 | 2.12 | 0.934 |
| I | 1 | 2.01 | 0.926 |
| I | 2 | 2.12 | 0.935 |
| II | 1 | 2.05 | 0.928 |
| II | 2 | 2.04 | 0.933 |
| III | 1 | 1.93 | 0.928 |
| III | 2 | 1.94 | 0.933 |

## 3.3 Automation of the recovery process

For the mechanical recovery methods performed in the above experiments to be feasible for a high volume of LCD, automation of some or the entire process is essential. Such an automated process must be capable of handling cleaning off the liquid crystal from substrates after separation and drying in preparation for mechanical treatment. Other factors that must be accounted for are the condition of the substrate post separation, identification of the ITO rich surface and number of passes during the brushing process. A proposed schematic of an automated recovery process is shown in Figure 12.

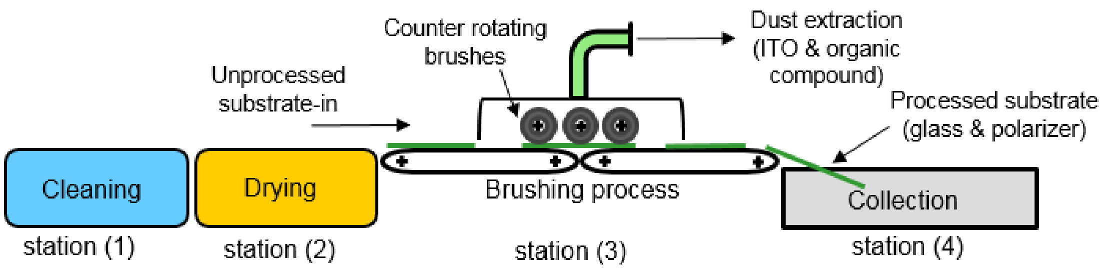


**Figure 12.** Automated recovery scheme.

The separated LCD substrate is cleaned in an acetone bath - station (1), next it is air dried - station (2) to remove fluid prior to the brushing - station (3) the brushing process is performed atop a vacuum conveyor system by multiple brushes in sequence combined with dust extraction systems. The brush substrate is collected - station (4) for subsequent separation of the glass and polarizer. In the automated process, the amount substrate that can be processed depends on the brush length and working area. From the brushing Experiment for LCD5 length of the diagonal 57.5 cm, length 48.5 cm, width 31.0 cm, the weight of 0.590 kg per panel was processed in 140 seconds using 20 cm wide roller 3 passes per substrate. For a one-meter brush length, a system consisting of three brushes can process 90 cm wide substrate in one-sixth of the time for the same sized LCD in a single pass, assuming 90% of the brush length is in contact with the substrates.

### 3.3.1 Investment cost estimates

Estimates for the capital investment for recovery scheme which includes the drying, brushing and collection stations is determined by vendors of similar systems. Two types of machines suitable for the brushing include industrial wide belt sander and the dual drum sander. Both machines require modifications to enable processing substrate thickness within 0.7 – 1 mm range. The tolerance requirement for the thickness in this application is expected to increase the cost of the standard wide belt sander by as much as 500 percent. Table 12 shows cost estimates for industrial scale recovery equipment sourced in Europe and China including the installation.

Table 12. Investment estimates for industrial recovery

| **Equipment** | **Capacity** | **Power** | **Thickness** | **Cost (€)** | **Modifications** |
|---|---|---|---|---|---|
| Wide belt sander | 430 x 630 mm | 5.5 kW | 3-160 mm | 52,600.00 | 0.7 -1mm |
| Tunnel dryer | 600 x 8000 mm | 17 kW | | 3,895.00 | Lower power |
| Vacuum/Blotter | 5200 m3/h | 4.0 kW | | 700.00 | |
| Total Fixed cost (TFC) | | | | 57,195.00 | |
| Installation | | | 10 % of TFC | 5,719.50 | |
| Excluding cleaning equipment & shipping | | | **Total cost** | 62,914.50 | |

### 3.3.2 Treatment cost estimate by methods.

The main portion of the operational cost of an industrial scale indium recovery process is the energy consumption by the processing equipment. An estimate for the energy consumption is based on machine power rating, the price of power per hour. For a system including the tunnel dryer, industrial wide belt sander and the industrial dust extraction/blotter.

To process 1 $m^2$ of the substrate, the estimated cost for treatment is computed as follows:

Energy consumption estimate (kWh) = Power (kW) x used time (h) (2)

Cost estimate (¢) = energy consumption (kWh) x Price (¢/kWh)

Electricity price (¢/kWh) = 20

Table 13. Energy consumption and cost estimates for the processes

| **Apparatus** | **Power (kW)** | **Time (h)** | **Consumption (kWh)** | **Costs (¢/m$^2$)** |
|---|---|---|---|---|
| Heat treatment 300 ºC | 2.67 | 0.5 | 1.335 | 26.7 |
| Heat treatment 600 ºC | 5.33 | 0.5 | 2.665 | 53.3 |
| Ind. Sanding machine | 5.5 | 0.02 | 0.11 | 2.2 |
| Ind. Blotter | 4 | 0.02 | 0.08 | 1.6 |
| Tunnel dryer | 17 | 0.02 | 0.34 | 6.8 |
| Plasma treatment | 1 | 0.025 | 0.025 | 0.5 |
| Compressed air | 1 | 0.025 | 0.025 | 0.5 |

The estimate for the drying process is based on a 17kW tunnel dryer with dimensions 2.4m by 0.6m having a heated length of 1.5m and minimum conveyor speed of 1.4m/min

The tunnel dryer is estimated to dry 1m$^2$ of LCD as follows:

Drying capacity (m$^2$/min) = Conveyor width (m) * min. speed. (m/min)
= 0.6 * 1.4 = 0.84 m$^2$/min

By proportional estimates 1 m$^2$ of substrate is can be dried in 1.19 minutes neglecting geometry limitations. This is equivalent to 0.02 hour of used time.

Cost estimate (¢) = 17kW * 0.02 h * 20 (¢/kWh) = 6.8 ¢ per 1m$^2$

Cost for heat treatment was estimated according to the equipment used in the experiment. A 12kW oven capable of attaining maximum temperature of 1350 ºC in an hour was used. The substrates were heated for 30 minutes at temperatures 300 ºC and 600 ºC. Oven capacity is 0.5m x 0.5m x 0.5m which and it is assumed to fit 1m$^2$ of CF+TFT substrates per treatment. The hypothesis is that that the oven will achieve the set temperature points using only 2.67kW and 5.33kW respectively for 30 minutes respectively.

Power consumption (300 ºC) = (12kW * 300 ºC) / 1350 ºC =2.67 KW
Cost estimate (¢) = 2.67 kW * 0.5 h * 20 (¢/kWh) = 26.7¢ per 1m$^2$

Combining the different pre-treatment as described in methods, the cost of recovery for 1 $m^2$ of substrate is calculated as a sum of treatment costs (₵/$m^2$) for the combination of methods tested. The costs of process requiring heat treatment are 30.5 and 57.1 ₵/$m^2$ respectively. The high consumption of the tunnel dryer is based on the rated power of similar systems. Table 14. shows the cost according to extraction approach.

*Table 14. Estimated recovery costs by method.*

| **Industrial extraction of indium combining different pre-treatment** | | | | |
|---|---|---|---|---|
| **Apparatus** | **Treatment** | | | |
| | Brush | Plasma & Brush | Heat 300 ºC & Brush | Heat 600 ºC & Brush |
| Oven | X | X | 26.7 | 53.3 |
| Plasma treatment | X | 1.0 | X | X |
| Tunnel dryer | 6.8 | 6.8 | X | X |
| Sanding machine | 2.2 | 2.2 | 2.2 | 2.2 |
| Blotter | 1.6 | 1.6 | 1.6 | 1.6 |
| Total (₵/$m^2$) | 10.6 | 11.6 | 30.5 | 57.1 |

Plasma treatment value in the table includes plasma generator (FG 5001) and plasma head (RD 1004) used in the experiments and compressed air required for treatment. The cost of treatment increases 1 ₵/$m^2$ when the plasma treatment is combined with brushing while the cost increases between 3 - 6 times with heat treatment. The heat treatment approach however does not require the tunnel drying stage since all solvent including liquid crystals are vaporized by the treatment.

### 3.4 Analytical methods

Elemental constituents of the substrates pre-treatment and post-treatment were analysed using a scanning electron microscope (SEM) to determine by qualitative and quantitative energy dispersive spectroscopy - EDS the metal content of the reference and treated substrates. This is followed by chemical analysis of the treated and reference substrate. Samples of black powdered material obtained from three (3) different LCD panels post mechanical treatment are subjected to chemical extraction process followed by precipitation of the metal content.

### 3.4.1 SEM analysis

Energy dispersive X-ray Spectroscopy (EDS) is a qualitative and quantitative microanalytical technique that can provide information on the chemical composition of a sample for elements with atomic numbers greater than 3. Electrons from an electron beam focused on the sample penetrates the sample and interacts with its constituent atoms. Characteristics X-rays and background X-rays generated because of the electron interactions are detected by an energy dispersive detector. Both rays superimposed is displayed as a spectrum of X-ray count versus X-ray energy and mapped against pre-stored values of known isotopes for identification. In Qualitative analysis, the elements present in the sample are identified using the spectrum of the characteristic X-ray peaks alone. The LCD substrate is stable under high vacuum (25 MPa) and not susceptible to deterioration under the electron beam so the acceleration voltage is selected as 15 kV, however 7 kV acceleration voltage was also used to investigate the effect of dirt/impurities on the substrate surface to detection. Using the high acceleration voltage ensured that higher energy K and L- band electrons are used in the identification. In the quantitative analysis, the concentrations of major and minor elements wt.% in different phases is calculated based on a standard reference. The detection limit for the SEM-EDS is in the range of 0.1-0.5 wt.% depending on the composition of the sample being analysed.

### 3.4.2 Chemical extraction process

The recovered dust can be leached using common mineral acid within technically feasible conditions. Depending of the purity of the "black mass" and selectivity of the cementation, it is possible to recover pure indium metal directly from the leachate, and when required, the leachate may be further purified by solvent extraction (T. Huhtanen, 2017.)

### 3.4.3 Wet combustion + ICP MS

The metal content in both the reference LCD substrates and treated substrates were analysed by wet combustion and ICP-MS. The substrate is first manually grinded then digested at high temperature (250 ºC), and high pressure (40 bar), with the aid of ultrasound and microwaves in the Device Milestone MA149. This liberates all the metals to the solution leaving only glass in the solid form. The aqueous solutions were analysed with ICP-MS (Agilent 7900) after diluting them with 1 wt. -% $HNO_3$. This provides quantitative data on the metal composition of the substrates.

# 4 RESULTS AND ANALYSIS

An analysis of the processed substrate appearance, the material composition of the substrate after processing, chemical composition of the recovered materials, and comparison of the pre-treatment methods is presented in this section. The composition of the substrate is determined from selected pieces of tested samples while the expected recovery percent of target material is evaluated based on the mass density of ITO on treated samples.

## 4.1 Experimental results of pre-treatment

Two pre-treatment methods that were performed, heat and atmospheric plasma treatment. Heat treatment was performed at two temperature points for two sets of LCD1 samples while plasma treatment was for a set of LCD2 samples.

### 4.1.1 Results of heat treatment

The observations for heat treatment show loss in material due to vaporization for CF samples heated up to at 600 ºC. Although literature indicates that ITO can withstand heat above the set temperature, the thin layer thickness of the ITO LCD coupled with the underlying organic material having lower decomposition temperature compared has resulted in co-vaporization of ITO particulates with the organic material. Substrate treated at 300 ºC showed fewer material losses. Figure 13 shows the effect of heat treatment to ITO layer for CF substrate. (a) The reference substrate sample and (b) heat treated sample of the same substrate. The heat-treated sample shows area of co-vaporization and patches of decomposed material.

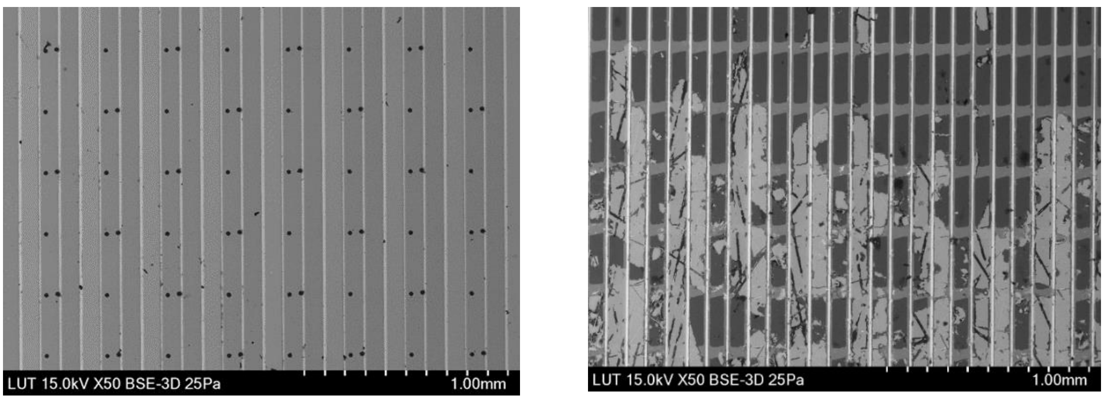


**Figure 13.** SEM image of the ITO surface LCD1 (a) untreated substrate (b) heat treated substrate 600 ºC

The composition map of the heat-treated sample shows a zero-indium content in the vaporized area while the patches of non-vaporized area have a weight of up to 43 percent.

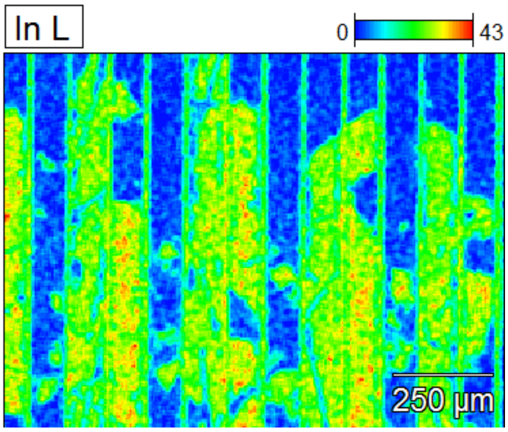


**Figure 14.** Indium content of heated CF substrate, temperature 600 ºC.

In the case of TFT substrate, heat treatment up to 600 ºC had less impact on the ITO layer. The ITO layer in TFT substrate behaves like bulk ITO and so high the temperature modifies surface structure. Vaporization was undetected in TFT as can be seen from the composition map. Although indium content on TFT is lower compared with CF, most area of the substrates has the ITO layer intact after heat treatment.

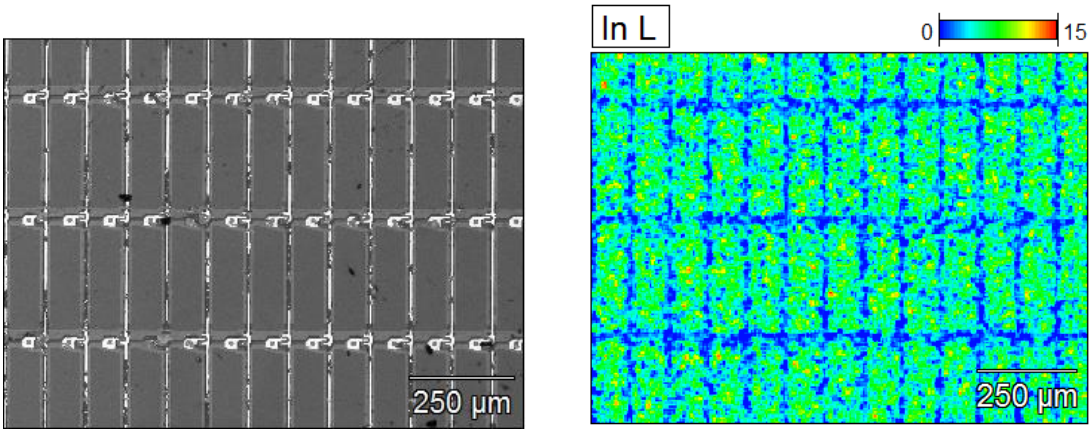


**Figure 15.** Heat treated TFT (a) BSE image of substrate 600 ºC (b) indium composition map 600 ºC.

Heat treatment also added a level of complication to the recovery process, glass substrates were in poorer conditions post treatment. Some of the ITO bearing material is also lost due to handling after 30 minutes of heat treatment. The time factor in this experiment varied considerably compared with the plain brushing process, as there was lower friction between heat treated glass and the working platform. The propensity for cracking increased significantly during processing. The glass substrate also proved difficult to handle once the polymeric polarizer material has been decomposed by heat. This experiment was performed using only the handheld grinder. During the grinding, it was observed from visual inspection of the substrate that the P60 abrasive had little to no effect on either substrate, P80 was effective for only CF substrates and P100 was most effective for both substrates.

4.1.2 Results of plasma treatment

Plasma treated samples exposed to for durations of 1, 2, and 5 seconds had different levels of deterioration of the ITO layer in the case of CF substrates. The plasma had the effect of breaking down the ITO. Similar results encountered in the heat treatment with loss of ITO material but in this case, material was blown away due to air delivered during the plasma process. Empirical observations of the composition maps of the samples showed a reduced presence of indium compared with the reference. Figure 16. Plasma treated CF substrates.

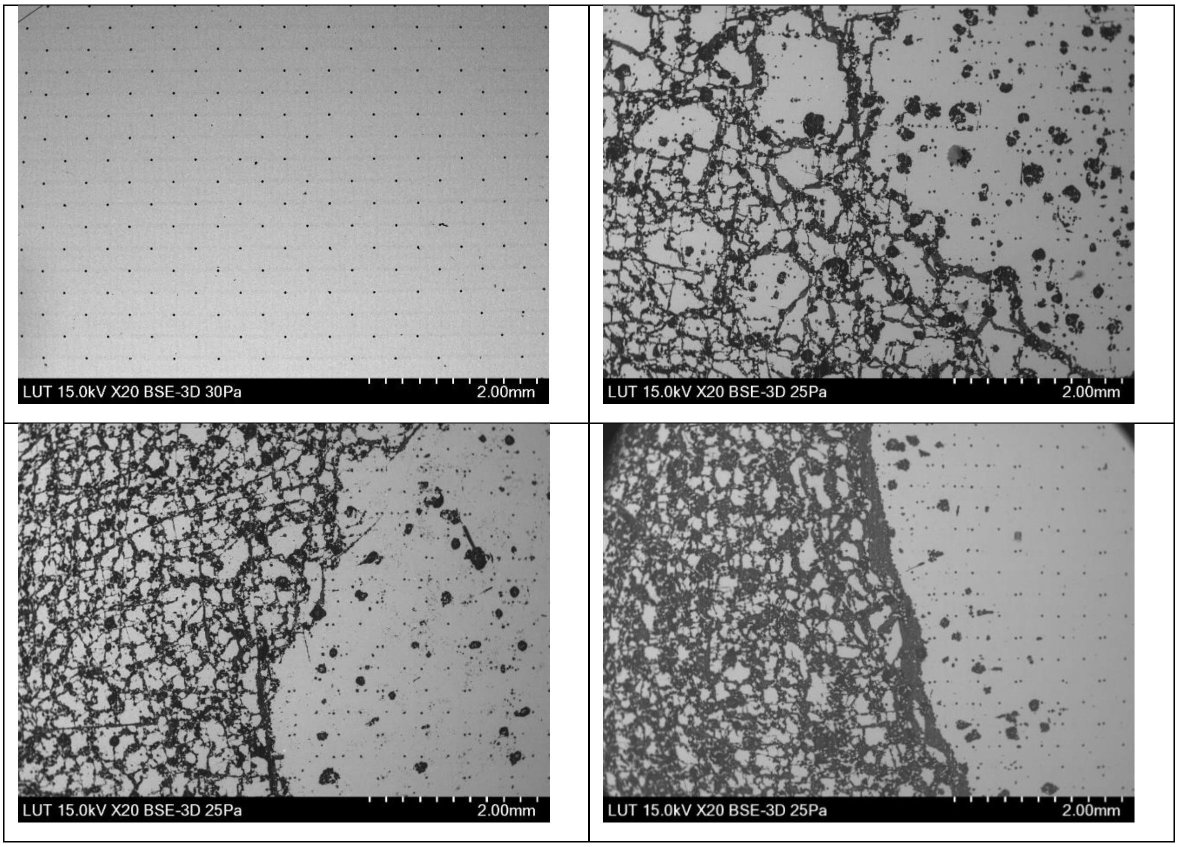


**Figure 16.** CF substrate (a) untreated sample. Plasma treated sample (b) 1 s top-right, 2 s bottom-left and 5 s bottom-right.

Plasma treatment of TFT substrate for similar duration produced a different result. The ITO layer was unmodified after by the treatment, while transistor circuits on of the TFT were broken. This could be due to the shorting of the transistor circuit by electric arcs of the plasma. Figure 17 show plasma treated TFT sample. The ITO layer remained intact, with no noticeable changes to the surface structure compared with the CF samples. However, the image on the left obtained at reduced power indicates the presence of the liquid crystal residue on the surface from the cleaning process.

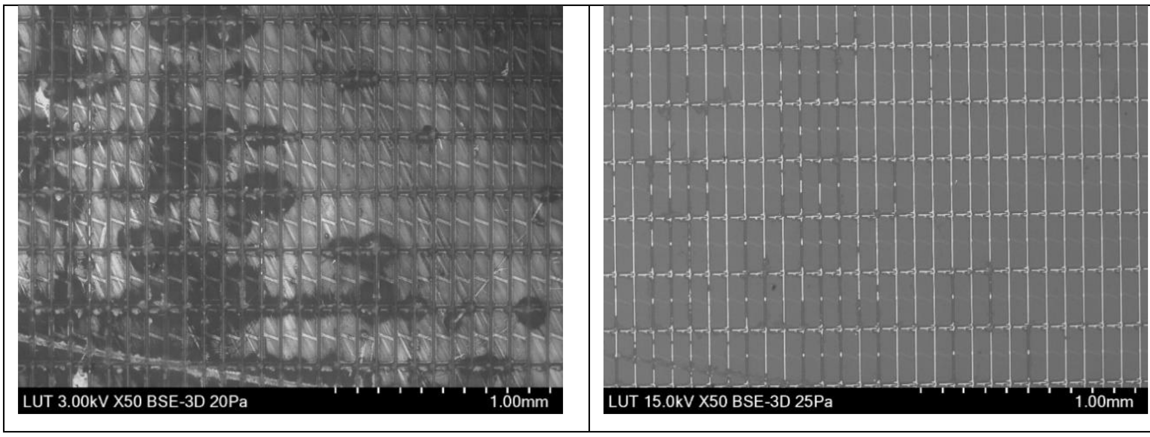


**Figure 17.** Plasma treated TFT substrate 5 seconds exposure.

Samples exposed for 1- and 2- seconds respectively showed similar characteristics as the 5 seconds. From this, it was observed that plasma treatment is ineffective as a physical pre-treatment for TFT substrates.

### 4.1.3 Results of laser treatment

Laser treatment of TFT was not possible due to high reflectivity of the coating. CF substrate was assessed to determine the impact of the treatment on the ITO layer. SEM images show the effect of laser exposure for the chosen treatment parameters. The sample shows a complete vaporization of the ITO layer leaving the organic material partially modified. However, methods for recovering the vaporized ITO is an aspect that needs to be further study for laser treatment to be feasible. Figure 18. shows a reference sample of the CF substrate and laser treated samples with bright ITO patches.

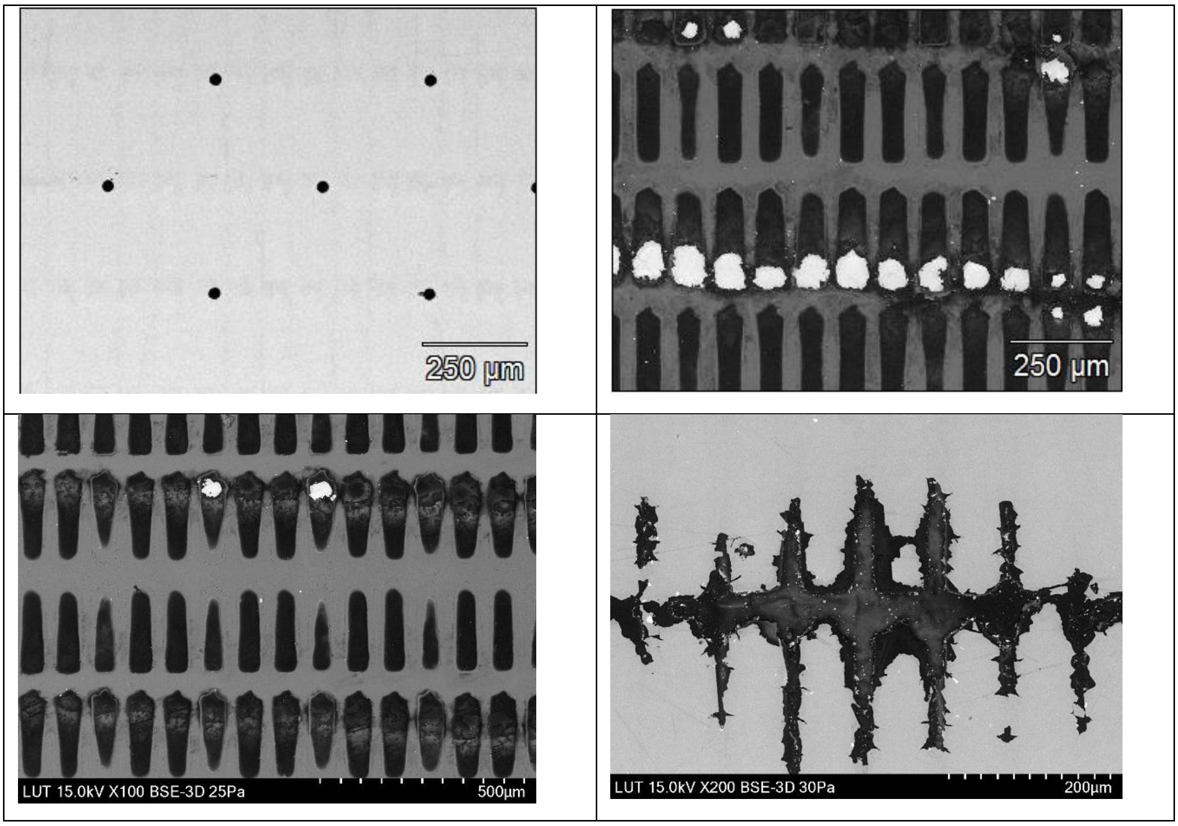


**Figure 18.** BSE image of untreated sample (top-left), laser treated 200 W, 400 mm/s (top-right), laser treated 200 W, 300 mm/s (bottom-left) and 200 W, 500 mm/s (bottom right).

Treatment at a speed of 300 mm/s produced a similar result as shown in the figure on the right. Increasing the speed of the laser scanning to 500 mm/s impacted the removal negatively, as the ITO layer remained on the sample with only a tiny fraction removed. Most of the indium content is vaporized from the path of the laser beam while the tiny patches show the areas with no beam interaction.

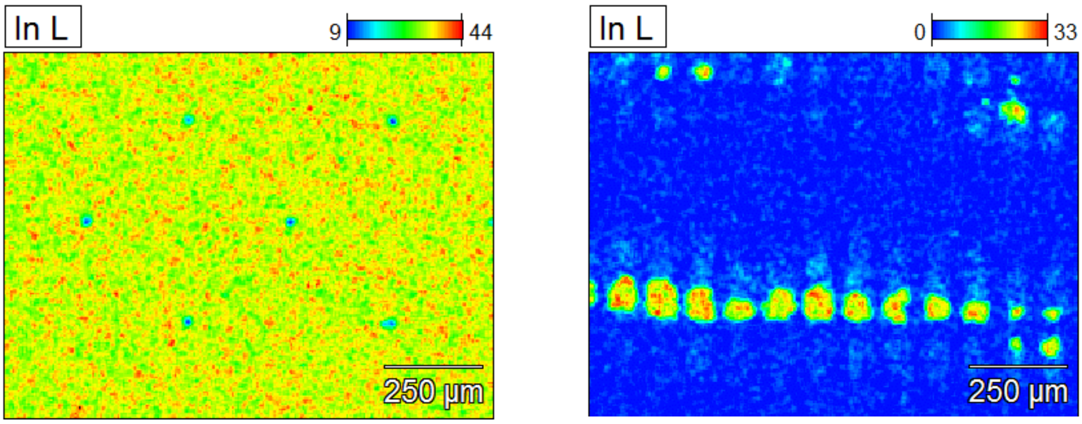


**Figure 19.** Indium composition of sample pre-treatment (left) and post-treatment (right).

## 4.2 Post treatment experiment

Post treatment experiments for substrates was brushing. Brushing was carried out on untreated, heat treated, and plasma treated samples. The materials recovered from the brushed samples were collected for chemical analysis.

### 4.2.1 Result of heat treatment and brushing/sanding

The number of tests presented reflect the effective combination of parameters in the recovery process. Images from SEM scanning provide information on the state of the substrate post brushing process. Heat treated samples treated at 300 ºC and 600 ºC were brushed using the hand sander. Figure 20 shows the result for CF (top) and TFT (bottom) substrates.

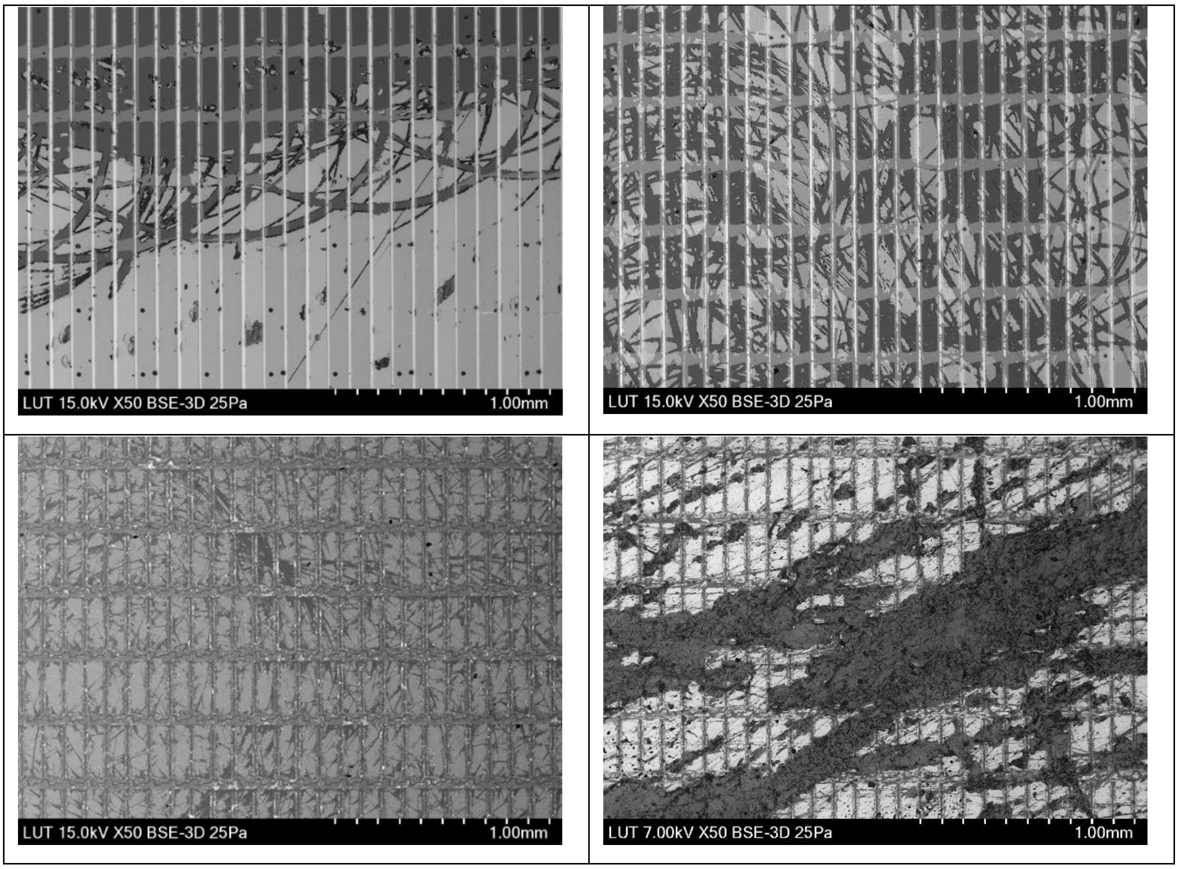


**Figure 20.** Heat treated and brushed (top) CF and (bottom) TFT, (left - right) 300 ºC and 600 ºC.

The efficacy of the sanding is noticed on the CF sample top-left treated at 300 ºC, the underlying organic material is not completely decomposed by heat and ITO was easily removed during the sanding process. The sample treated at higher set temperature on the other hand had most areas intact. The TFT samples heated in at the two set temperature points showed similar characteristics. Sanding using aluminium-oxide abrasive was ineffective, changing to silicon abrasive resulted in gouging the substrate and removal of the glass which is an undesired result.

### 4.2.2 Result of plasma treatment and brushing

Brushing the plasma treated samples, it was observed that for the CF glass, ITO layer was easily recovered. The plasma both the ITO layer and the underlying organic material which could already be removed by scratching. The TFT substrate however was harder to abrade. There were minor scratches on the TFT surface after brushing, and broken conductor lines but ITO layer mostly remained intact. Figure 21. Plasma treated and brushed samples.

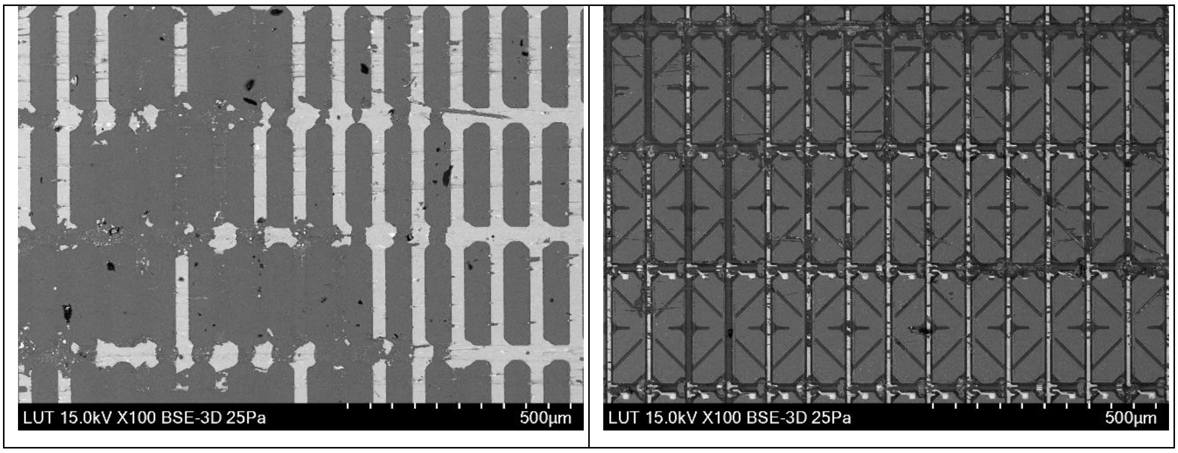


**Figure 21.** Plasma treated and brushed CF (left) and TFT (right).

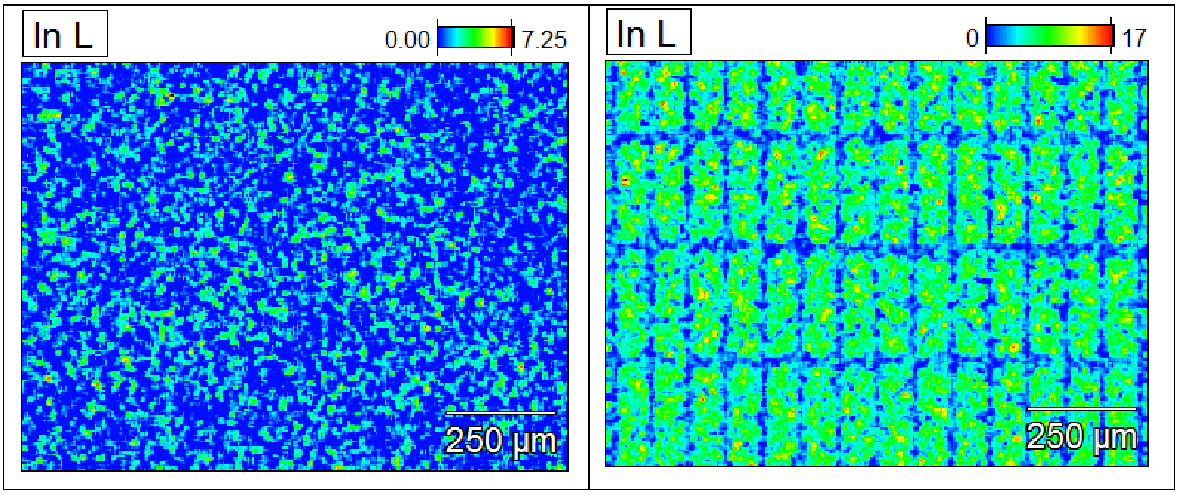


**Figure 22.** Indium composition for plasma treated brushed samples CF and TFT.

The ITO layer in the TFT is unaffected by the Plasma. A combination of plasma treatment and brushing either does not impact the ITO layer. When compared with the CF substrates most of the ITO is unaffected by the plasma and brushing. Increased treatment time of 5 second produced similar results as shown in Figure 22.

## 4.3 Result of brushing without pre-treatment

The recovery process without pre-treatment relied only on the abrasive. This method produced a similar result as the plasma pre-treated samples with respect to the removal efficacy without the associated loss of ITO material. This experiment was performed on samples LCD1 and LCD5.

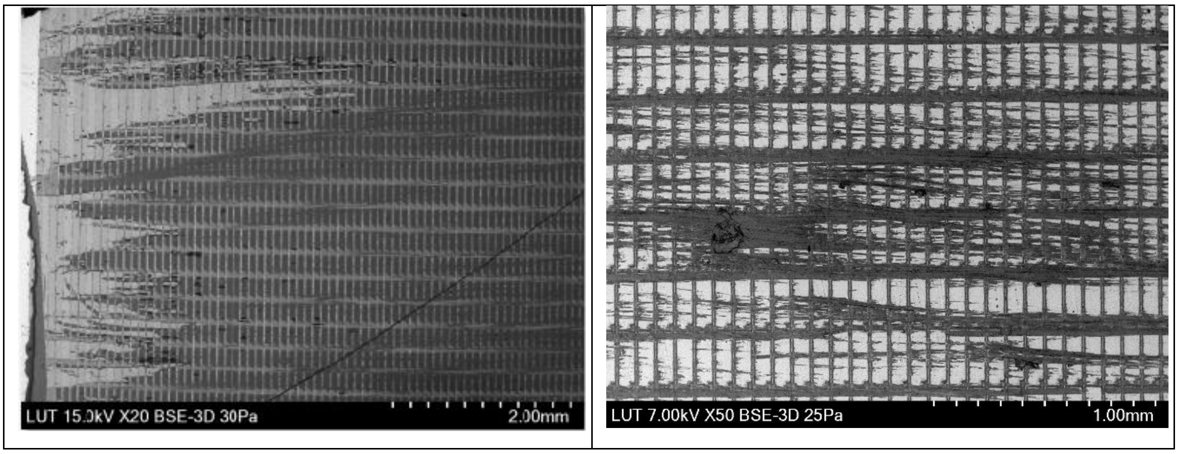


**Figure 23.** Untreated brushed CF (left) and TFT (right) substrates.

A magnified image of the CF substrate captures a region mildly brushed. The underlying glass substrate (4) can be identified as area where the organic material and ITO layer is completely scraped. The ITO layer (1) atop of the (2) organic and (3) passivation layers is depicted in the image. Figure 24. Magnification of the brushed untreated TFT substrate showed similar results as the plasma treated TFT substrate.

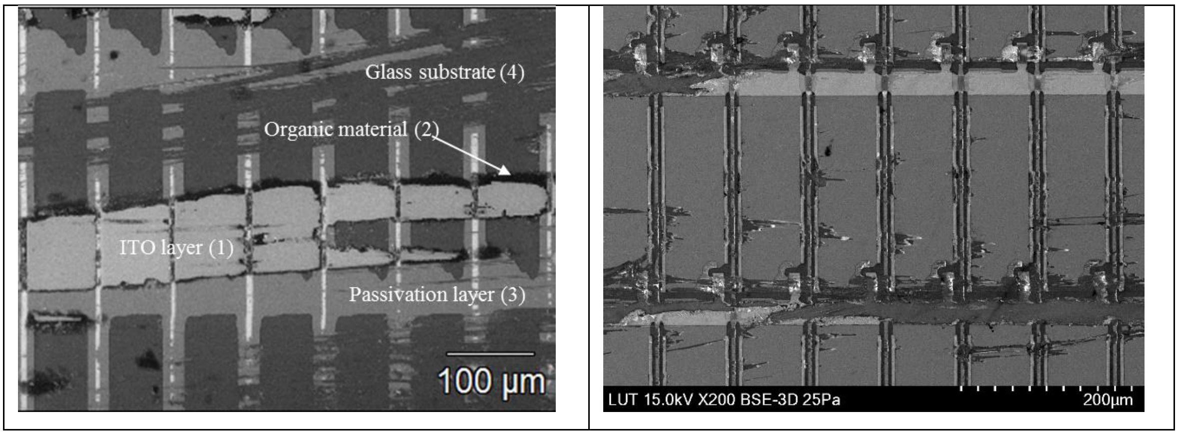


**Figure 24.** Untreated CF and TFT substrate showing material layers.

Composition image analysis for the CF (left) and TFT (right) substrates, shows indium content Figure 25. The weight of indium in the abraded area is 0 while the un-abraded region shows a high weight up to 37. Indium content in the TFT (right) which is usually low in value is shown sparsely distributed. Other elements that are contained in the substrates are not shown in the image.

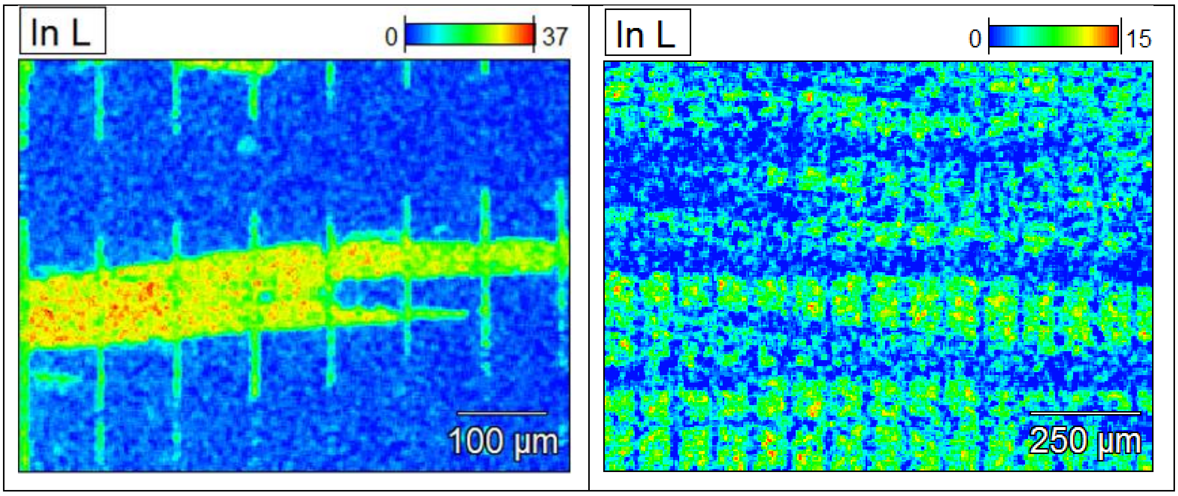


**Figure 25.** Indium composition of brushed CF and TFT substrate.

## 4.4 Evaluation of the treatment methods

To assess the methods utilized in recovery we establish the basis for comparison as follows; the treatment process, the ease of material handling, time consumed for processing a single LCD substrate, amount of recovered material by method, material composition.

### 4.4.1 Treatment process

The pre-treatments prior to brushing were processes chosen to improve the recovery of the ITO rich material from the substrates. When comparing heat treatment and plasma treatment regarding process viability, plasma treatment had the most promising viewpoint. Both treatments add one or more new stages to the recovery process, but heat treatment had the problem of debris accumulation from polarizer decomposition and remnants of the adhesive when the polarizer is removed before treatment. The removal of the polarizer creates a new problem for handling after heat treatment. Most LCD substrates are cracked, and the attached polarizer film acts as support during the mechanical process. The removal of the film prior to or due to heating creates the problem of handling, identification of the ITO bearing surface of substrate and excessive crack propagation during brushing. These problems are absent in plasma treatment since treatment affects only the surface exposed to the plasma.

### 4.4.2 Processing time

In the heat treatment, processing time increased due to required cooling time for heated substrate. Substrate remained in the kiln over four hours for cooling after achieving the desired temperature. Plasma treatment however had a shorter processing time, less than one minute for each LCD2 samples treated. Treatment time depends on the nozzle diameter and the surface area treated. Substrate proceeded to the next processing stage immediately after plasma treatment which is vital for automatization.

### 4.4.3 Comparison of recovered extracts and economics of the recovery

To ascertain the effectiveness of the pre-treatment, the amount of recovered material, Yield (g), the indium content of recovered dust (g/kg) for the pre-treated and untreated is compared. The number of samples treated, and the area of the samples is different for LCD1 and LCD2. So, a comparison is made per unit area of the samples processed in Table 16. LCD1 untreated, heat treated and LCD2 untreated and plasma treated and LCD 5 untreated.

$$\text{Yield [column 6] (mg/cm}^2\text{)} = \text{Yield [column 5] / Number of LCD * Area} \qquad (3)$$

*Table 16. Comparison of pre-treatment and untreated mechanical process.*

| Sample | Treatment | No. | Area ($cm^2$) | Yield (g) | Yield ($mg/cm^2$) | Indium g/kg |
|---|---|---|---|---|---|---|
| LCD1 | Heat 300 ºC | 15 | 489.5 | 3.12 | 0.425 | 146.76 |
| LCD1 | Heat 600 ºC | 12 | 489.5 | 2.59 | 0.440 | 141.76 |
| LCD1 | Untreated* | 25 | 489.5 | 2.32 | 0.190 | 155.85 |
| LCD2 | Plasma | 28 | 740.25 | 10.62 | 0.512 | 88.57 |
| LCD2 | Untreated | 18 | 740.25 | 5.66 | 0.425 | 71.47 |
| LCD5 | Untreated | 15 | 1503.5 | 8.68 | 0.385 | 125.36 |

***** Outlier: recovered using hand sander/including TFT

The material composition of the powered samples determined from leaching is shown in Table 17. The indium to tin content is in ratio 10:1 according to standard ITO chemical composition. The iron content the main contaminant of the indium in conventional extraction methods is low according to this result.

The purity of the recovered material was evaluated to be above 93% for the applied methods. This was calculated by as follows:

$$P_{In} = \frac{C_{In}}{\sum_i C_i} * 100\ \% \quad (4)$$

Where $C_{In}$ Concentration of indium in the leachate, mg/L

$C_i$ Concentration of metal '*i*' in the leachate, mg/L

*Table 17. Metal composition of powdered material recovered from LCD substrates.*

| # | Method | Composition of elements in dust recovered g/kg | | | | | | wt. % In & Sn | Indium Conc.% |
|---|---|---|---|---|---|---|---|---|---|
| | | In | Sn | Al | Fe | Cu | Zn | | |
| LCD1 | Brushing[1] | 155.85 | 15.58 | 2.66 | 1.20 | 5.41 | 1.64 | 94.02 | 15.58 |
| LCD2 | Brushing[2] | 71.47 | 8.96 | 7.46 | 5.29 | 3.15 | 1.56 | 82.16 | 7.14 |
| LCD5 | Brushing[2] | 125.36 | 16.05 | 6.67 | 1.11 | 5.92 | 0.61 | 90.81 | 12.54 |
| LCD1 | Heat$^{1}_{a}$ | 141.76 | 17.92 | 4.13 | 1.10 | 5.24 | 0.65 | 93.49 | 14.18 |
| LCD1 | Heat$^{1}_{b}$ | 146.76 | 18.31 | 3.66 | 0.79 | 5.13 | 0.86 | 94.05 | 14.68 |
| LCD2 | Plasma[2] | 88.57 | 11.12 | 5.48 | 0.85 | 3.99 | 0.42 | 90.27 | 8.86 |

Sanding[1], Lamella roller[2], a =600 ºC, b = 300 ºC.

The indium content in the dust sample for untreated LCD2 is 19% lower in comparison with plasma treated sample and the untreated LCD2 dust sample has a highest iron content 5.29 g/kg of the samples tested. The high iron content is not replicated in the untreated LCD5 dust sample extracted using a similar process. The average metal composition of LCD samples used in study as measured by wet combustion and ICP-MS method is given in mg/kg Table 18.

*Table 18. Composition of LCD substrates reference samples in mg/kg.*

| # Reference | In | Sn | Al | Fe | Cu | Zn |
|---|---|---|---|---|---|---|
| LCD1 | 369.47 | 49.33 | 378.73 | 3.13 | 11.67 | 3.15 |
| LCD2 | 273.89 | 38.96 | 586.92 | 2.56 | 5.76 | 24.95 |
| LCD5 | 422.93 | 52.56 | 230.73 | 1.58 | 16.11 | 3.93 |

An evaluation of the average composition of pre-treated substrates shows the effect of increased temperature on the ITO layer. The sample treated to 600 ºC resulted in severe losses of the ITO material. Average indium content was 94.00 mg/kg, implying over 70% loss compared with 300 ºC treatment Table 19. The content of the plasma treated LCD2 substrate however showed higher content than the reference.

*Table 19. Metal composition of treated substrates pre-brushing.*

| # Treated | Method | Composition of metal elements mg/kg | | | | | |
|---|---|---|---|---|---|---|---|
| | | In | Sn | Al | Fe | Cu | Zn |
| LCD1 | Heat[1]a | 94.00 | 21.14 | 348.69 | 2.16 | 0.91 | 0.22 |
| LCD1 | Heat[1]b | 351.13 | 56.36 | 334.73 | 7.54 | 6.00 | 1.84 |
| LCD2 | Plasma[2] | 362.79 | 47.86 | 475.29 | 3.01 | 9.26 | 19.26 |

Sanding[1], Lamella roller [2], a =600 ºC, b = 300 ºC.

Post mechanical extraction, substrates showed minute quantities of residual indium Table 20. Substrate LCD1 treated at 600 ºC unexpectedly showed the highest amount of residual indium.

*Table 20. Metal composition of treated and untreated substrates post-brushing.*

| # | Method | Composition of metal elements mg/kg | | | | | |
|---|---|---|---|---|---|---|---|
| | | In | Sn | Al | Fe | Cu | Zn |
| LCD1 | Brushing[1] | 14.19 | 8.48 | 432.59 | 3.51 | 0 | 4.36 |
| LCD2 | Brushing[2] | 23.80 | 15.29 | 735.66 | 4.70 | 0 | 1.61 |
| LCD5 | Brushing[2] | 17.85 | 3.26 | 263.08 | 2.34 | 0 | 2.91 |
| LCD1 | Heat[1]a | 56.05 | 16.52 | 366.11 | 3.19 | 0 | 3.28 |
| LCD1 | Heat[1]b | 29.44 | 65.65 | 2071.96 | 20.58 | 0 | 5.09 |
| LCD2 | Plasma[2] | 10.44 | 3.49 | 387.09 | 3.01 | 1.36 | 1.17 |

Sanding[1], Lamella roller [2], a =600 ºC, b = 300 ºC.

### 4.4.4 Comparison chemical analysis and theoretical indium content.

The theoretical indium content of the reference LCD substrates estimated based on ITO layer thickness of 150 nm on the LCD substrate is compared with the amount of indium obtained through chemical analysis Table 21.

*Table 21. Indium content of LCD by analysis method.*

| # | Area ($cm^2$) | Weight of LCD (kg) | Theoretical est. In mg/kg | Chem. analysis In. mg/kg |
|---|---|---|---|---|
| LCD1 | 489.5 | 0.201 | 469.6 | 369.47 |
| LCD2 | 740.2 | 0.292 | 489.2 | 273.89 |
| LCD5 | 1503.5 | 0.590 | 491.7 | 422.93 |

The chemical analysis values can be 14% – 44% less than the estimated theoretical value, however the chemical analysis results are regarded as most accurate.

The expected concentration of indium from the LCD substrates according to the difference between reference content and the residual content including losses due to the utilized mechanical method and pre-treatments is shown in column 5 of Table 22. The expected yield (mg) is a product of the mass treated and the expected concentration. The actual yield is then evaluated as a product of the concentration of extracts and the mass of LCD substrate treated.

*Table 22. Expected yield of indium based on chemical analysis concentration vs extraction methods.*

| # | Mass (kg) | Treatment | Reference concentration (mg/kg) | Residual concentration (mg/kg) | Exp. extract concentration (mg/kg) | Expected yield (mg) |
|---|---|---|---|---|---|---|
| LCD1 | 5.025 | Untreated | 369.47 | 14.19 | 355.28 | 1785.28 |
| LCD2 | 5.256 | Untreated | 273.89 | 23.80 | 250.09 | 1314.47 |
| LCD5 | 3.924 | Untreated | 422.93 | 17.85 | 405.08 | 1589.53 |
| LCD2 | 8.176 | Plasma | 273.89 | 10.44 | 263.45 | 2153.96 |
| LCD1 | 3.015 | Heat-300 | 422.93 | 29.44 | 393.49 | 1186.37 |
| LCD1 | 2.412 | Heat-600 | 422.93 | 56.05 | 366.88 | 884.91 |

The macro yield in percentage was evaluated to shows the fraction of indium recovered by mechanical methods over the expected yield Table 23. The result for macro yield shows a significant difference when compared with the expected yield. The difference could be ascribed to heterogeneity of the samples treated since indium content in the treated LCD’s could vary by the generation of the substrate and the different manufacturers. Moreover, dust losses during brushing which was significant and variations in the chemical analyses could also impact these results.

*Table 23. Macro yield of indium from extract excluding losses.*

| # | Mass (kg) | Treatment | Expected yield (mg) | Chemical analysis (mg/kg) | Macro yield (mg) | Macro yield (%) |
|---|---|---|---|---|---|---|
| LCD1 | 5.025 | Untreated | 1785.28 | 155.85 | 783.14 | 43.86 |
| LCD2 | 5.256 | Untreated | 1314.47 | 71.47 | 375.64 | 28.58 |
| LCD5 | 3.924 | Untreated | 1589.53 | 125.36 | 491.91 | 30.95 |
| LCD2 | 8.176 | Plasma | 2153.96 | 88.57 | 724.15 | 33.62 |
| LCD1 | 3.015 | Heat-300 | 1186.37 | 146.76 | 442.48 | 37.30 |
| LCD1 | 2.412 | Heat-600 | 884.91 | 141.76 | 341.92 | 38.64 |

The cost of heat treatment costs is noted to be beyond tolerable limits. The value of indium per square-meter is evaluated based on indium recovered using plasma pre-treatment + brushing at 11.6 ¢/m$^2$ and brushing only at 10.6 ¢/m$^2$. Using the market price of indium $ 360/kg in 2017 sourced from minerals commodity summaries 2018. Column 8, Table 25. Value ($/m$^2$) is the product of recovered indium (mg/m$^2$) and price ($ 360/kg).

*Table 25. Value of indium recovered by selected methods.*

| # | Area (m$^2$) | Weight / unit (kg) | Method | Weight (kg/m$^2$) | Chem. analysis (mg/kg) | Indium (mg/m$^2$) | Value ($/m$^2$) |
|---|---|---|---|---|---|---|---|
| LCD1 | 0.04895 | 0.201 | untreated | 4.106 | 155.85 | 639.92 | 0.23 |
| LCD2 | 0.07402 | 0.292 | untreated | 3.945 | 71.47 | 281.95 | 0.10 |
| LCD5 | 0.15035 | 0.590 | Untreated | 3.924 | 125.36 | 491.91 | 0.18 |
| LCD2 | 0.07402 | 0.292 | Plasma | 3.945 | 88.57 | 349.41 | 0.13 |

The quantity of indium (mg/m$^2$) recovered could be higher if the process is strictly controlled to mitigate losses thus increasing the value of recovered indium per square meter of glass substrate.

# 5 DISCUSSION

Several observations were made from the results of the experiments and over the course of the thesis. To identify the main benefits, results of the utilized methods are compared with the outcome of previous studies. The key performance indicators in indium recovery from LCD’s are the quantity, purity level of the material, the feasibility of the methods for large scale recovery.

Mechanical exfoliation (Wang S. et al, 2017) and mechanical stripping (L. Zhang et al. 2017) proposed for indium recovery can be compared with the mechanical extraction process applied in this work. Mechanical stripping involved removal of an indium rich glass fraction along with the liquid crystals, the stripping product is treated first by pyrolytic decomposition before chemical extraction of metals. The mechanical exfoliation test bed uses a negative vacuum lapping polisher on liquid crystal free substrate to achieve a similar result. Brushing as used in this work, is a dry process with negligible glass substrate recovered as co-product of the brushing. The amount of indium recovered per weight for different studies is summarized in the Table 25.

*Table 25. Comparison of amount of indium recovered by method.*

| Study | Method | Process | Indium wt.% |
|---|---|---|---|
| Zhang L, et al 2017 | Stripping and pyrolysis | wet | 7.95 |
| Wang S, et al 2017 | Negative pressure polisher | dry | 7.26 |
| This work | Untreated brushing | dry | 7.54 - 15.58 |
| This work | Heat pre-treatment | dry | 14.68 |
| This work | Plasma pre-treatment | dry | 8.86 |

Indium concentration increased to twice the values achieved in previous studies. The concentration of indium also varied according to the deposition characteristics of ITO layer. LCD2 samples had the lowest content of indium according to ICP-MS analysis of reference substrate, and it reflects in the concentration obtained by mechanical processing. Untreated LCD2 was concentrated 7.54 wt.% and the Plasma treated LCD2 8.86 wt.%. The plasma treatment resulted in a 1.32g/kg increase in concentration compared with the untreated. The residual LCD substrate in this work however has some remnant of the target material for both pre-treated and untreated samples. The high temperature point for heat treated substrates had high indium retention 56.05 mg/kg. Plasma treated, and untreated substrates retained 10.44 – 23.80 mg/kg of indium post brush. The amount retained is significant and further study is required to understand its impact on substrate utilization for other applications.

Comparing the mechanical extraction method used in this work to the comminution process in previous research, some of the advantages of the mechanical process includes lower amount of solvent required for the chemical extraction from powder and precipitation. The comminution process requires a large mass pulverized of glass substrate to be processed chemically in other to recover small amounts of indium, while the mechanical process reduces the mass of material fed to the chemical extraction process to one-hundredth weight of entire glass substrate. More so, it might be possible to avoid the efficient but expensive solvent extraction and purification step.

The purity of the recovered indium is also high at 93% due to low amount of iron, the major contaminant in the conventional process. Iron contamination in the conventional process can be due to ingress from the tooling during crushing. This is low in the applied methods since the abrasive materials used are iron free.

The pre-treatment methods applied in this work have not been used previously attempted in indium recovery. Heat treatment as utilized in this work achieved one purpose further reduction in the amount of material for chemical extraction as the organic layer below the ITO on CF was decomposed by the heat input. However, its impact is diminished when heating is carried out in an unsealed oven due to co-vaporization. Some of the ITO material is lost as effluents. These losses are absent in the pyrolytic recovery (Zhang L, et al 2017) and vacuum thermal carbonization (He Y., et al 2014) since vaporized materials are contained within a condensing chamber.

Next, suitable parameters for pre-treatment and mechanical extraction were established through the experiments. Suitable heat treatment temperature for CF substrates was established as 300 – 350 ºC. Increasing the temperature above this range results in an excessive vaporization of the underlying organic material, this was confirmed from SEM images of treated material. Heat treatment was observed not to be feasible for TFT as the examined temperatures failed to impact the recovery of powder from the substrate.
In the laser treatment, indium was not recovered as the indium evaporates. A possible method to collect the indium could be to capture the vaporized material in water. This

approach will depend on how well the vaporized material dissolves and how feasible it is to recover from the fluid.

Plasma treatment with three different time extents 1, 2 and 5 seconds showed that sufficient treatment was achieved at 1 - 2 seconds. TFT substrates treatment did not produce positive results even at the uppermost treatment time. The brushing process performed after heat and plasma treatment showed that higher grit abrasive is suitable for heat treated samples and lower grit abrasive for the untreated and plasma treated samples. The abrasive grit size for the brushing process was above 100 – 220 grits for heat treated sample and 80 grits for the plasma and untreated sample. The performance of the brushing process also varied by the machine types. The 3500 RPM constant speed of the wheeled sander used was suitable for both untreated and treated samples. Other brush speeds were not examined during the experiment so, this will require further investigation. The establish parameters are presented in Table 26.

*Table 26. Process parameters.*

| Process | Time | Abrasive | Grit size | Speed (RPM) |
|---|---|---|---|---|
| Heat 300 ºC | 30 mins. | Silicon based | P100- 220 | - |
| Plasma | 1 – 2 Sec. | Aluminium oxide | P80 - 100 | 3500 |
| Untreated | - | Aluminium oxide | P80 - 100 | 3500 |

Abrasive material also had impact on the recovery process, aluminium oxide-based abrasive was enough for untreated and plasma treated samples of CF, while silicon carbide-based abrasive performed better on the heat-treated samples. TFT substrate showed gouging with the change in abrasive material, with associated increase glass substrate removal.

# 6 CONCLUSSION

A mechanical method for recovering ITO rich material from end-of-life LCD screens with and without physical pre-treatment was studied in the laboratory using waste LCD screens. The methods relied findings by (T. Huhtanen, 2017) and publicly available literature. The key findings in recovery of ITO from LCD substrates are:

- A combination of atmospheric plasma pre-treatment and brushing is an effective method for improving indium concentration and recovery from LCD glass. Brushing using abrasive paper grit sizes P80 – 100 is effective to liberate the ITO layer on CF glass of LCD and a viable alternative to comminution.
- Indium recovered from samples was concentrated from 0.02 wt.% common in the conventional process to between 7.54 - 15.58 wt.% using the mechanical methods. Purity of the indium was up to 93 % and it had lower iron contamination as low as 0.72%.
- The plasma pre-treatment provided the best concentration for indium as plasma treated LCD2 substrate indicate a concentration of 88.6 g/kg and 71.4 g/kg for the untreated sample. The heat pre-treated LCD1 sample showed a reduced concentration 146.8 g/kg compared with untreated sample 155 g/kg. Indium recovered also varied by the characteristics of ITO layer on different LCD glass, this can influence output of the process in industrial scale recovery scheme.
- The methods applied were bench scale and so materials were carefully selected for treatment thus results may vary in the industrial scale application. For practicability, the LCD material must be presented with minimum damage. Separation of LCD into CF and TFT substrate to expose ITO surface including cleaning off liquid crystal material is an important step. The polarizer layer must be maintained intact and where it is damaged, alternative means of work holding needs to be developed.
- An industrial scale mechanical recovery process can be implemented using a production line approach. The pre-treatment process is implemented at the beginning of the line either automated or manually, wide belt sanding the main processing step is combined with a vacuum blotter for target material collection. While the glass residue is collected at the end of the line. Although the pre-treatment improves indium concentration, its impact in industrial scale recovery would be too minute to offset the cost of the step, so this could be excluded.

Some aspects that would be interesting for future work, application of brushing to multi-layered polymeric materials for separation of thin polymer films, determining specific machine parameters such as the feed rate, belt speed and contact pressure and other abrasive materials suitable for the brushing process in industrial scale equipment. The influence of a combined transverse and longitudinal brushing direction on the recovery and determination of the abrasive belt lifespan should be studied since tool wear behaviour for glass and other materials differ.

# 7 REFERENCES

Atif Alkhazaili, Mohammad M. Hamasha, Gihoon Choi, Susan Lu, Charles R. Westgate, 2015. Reliability of thin films: Experimental study on mechanical and thermal behavior of indium tin oxide and poly(3,4-ethylenedioxythiophene), In Microelectronics Reliability, Volume 55, Issues 3–4, 2015, Pages 538-546, https://doi.org/10.1016/j.microrel.2015.01.013.

Avanstrate, 2017. "*Chemical composition in mol.% mechanical properties of LCD - ITO glass.*" [webpage]. [accessed: 12.12.2017] available at: http://www.avanstrate.com/english/product/product_data.html

Boundy, T., Boyton, M. and Taylor, P., 2017. "Attrition scrubbing for recovery of indium from waste liquid crystal display glass via selective comminution". Journal of Cleaner Production, 154, pp. 436-444.

Cheol-Hee Lee, Mi-Kyung Jeong, M. Fatih Kilicaslan, Jong-Hyeon Lee, Hyun-Seon Hong, Soon-Jik Hong, 2013. Recovery of indium from used LCD panel by a time efficient and environmentally sound method assisted HEBM, In Waste Management, Volume 33, Issue 3, Pages 730-734, https://doi.org/10.1016/j.wasman.2012.10.002.

Danilo Fontana, Federica Forte, Roberta De Carolis, Mario Grosso,2015. Materials recovery from waste liquid crystal displays: A focus on indium, In Waste Management, Volume 45, 2015, Pages 325-333, https://doi.org/10.1016/j.wasman.2015.07.043

Desktop and computer display: a lifecycle assessment",2014 [online document]. [accessed: 12.12.2017] available at https://www.epa.gov/sites/production/files/2014-01/documents/computer_display_lca.pdf

European commission – COM, 2017. [online document]. [accessed:22.12.2017] available at: http://eur-lex.europa.eu/legal-content/EN/TXT/PDF/?uri=CELEX:52017DC0490&from=EN

Francesco Ferella, Girolamo Belardi, Antonella Marsilii, Ida De Michelis, Francesco Vegliò, 2017. Separation and recovery of glass, plastic and indium from spent LCD panels, In Waste Management, Vol:60, Pp:569-581. https://doi.org/10.1016/j.wasman.2016.12.030

Ghorannevis, Z., Akbarnejad, E. & Ghoranneviss, M., 2015. Journal of Theoretical and Applied Physics Volume 9, Issue 4, pp 285-290. https://doi.org/10.1007/s40094-015-0187-3

Glass properties, 2017. “Chemical composition and mechanical properties of LCD - ITO glass”. [webpage] [accessed 12.12.2017] available at: http://glassproperties.com/glasses/

Hasegawa, Hiroshi Hasegawa, Ismail M.M. Rahman, Yuji Egawa, Hikaru Sawai, Zinnat A. Begum, Teruya Maki, Satoshi Mizutani., 2013, Chelant-induced reclamation of indium from the spent liquid crystal display panels with the aid of microwave irradiation, Journal of Hazardous Materials, Vol: 254–255, Pages 10-17, https://doi.org/10.1016/j.jhazmat.2013.03.028

Hiroyuki Yoshida, Shamsul Izhar, Eiichiro Nishio, Yasuhiko Utsumi, Nobuaki Kakimori, Salak Asghari Feridoun, 2014. Recovery of indium from TFT and CF glasses in LCD panel wastes using sub-critical water, In Solar Energy Materials and Solar Cells, Volume 125, Pages 14-19. https://doi.org/10.1016/j.solmat.2014.02.009.

Huhtanen, T. 2017. Indium recovery from LCD-screens with continuous liquid-liquid extraction. Master’s thesis. Lappeenranta: Lappeenranta university of technology. Chemical separation processes.

Indium statistics and information, 2017. [webpage]. [Accessed 11.12.2017] available at https://minerals.usgs.gov/minerals/pubs/commodity/indium/

Jiaxu Yang, J., Teodora Retegan, T., Britt-Marie Steenari, B., Christian Ekberg, C., 2016, “Recovery of indium and yttrium from Flat Panel Display waste using solvent extraction”, In Separation and Purification Technology, Volume 166, 2016, Pages 117-124, https://doi.org/10.1016/j.seppur.2016.04.021.

Jiuli Ruan, Yuwen Guo, Qi Qiao, 2012. Recovery of Indium from Scrap TFT-LCDs by Solvent Extraction, In Procedia Environmental Sciences, Vol 16, pp 545-551. https://doi.org/10.1016/j.proenv.2012.10.075.

Kaihua Zhang, Bin Li, Yufeng Wu, Wei Wang, Rubing Li, Yi-Nan Zhang, Tieyong Zuo, 2017., “Recycling of indium from waste LCD: A promising non-crushing leaching with the aid of ultrasonic wave”, In Waste Management, Volume 64, 2017, Pages 236-243, https://doi.org/10.1016/j.wasman.2017.03.031.

Kaihua Zhang, Yufeng Wu, Wei Wang, Bin Li, Yinan Zhang, Tieyong Zuo, Recycling indium from waste LCDs: A review, 2015. In Resources, Conservation and Recycling, Volume 104, Part A, 2015, Pages 276-290. https://doi.org/10.1016/j.resconrec.2015.07.015.

Kopacek, B., 2010. Re LCD recycling and re-use of LCD panels, Proceedings of the 2010 IEEE International symposium on sustainable systems and technology, Arlington, VA, 2010, pp. 1-3. doi: 10.1109/ISSST.2010.5507735

LG recycling program, 2017. [webpage]. [accessed; 13.12.2017] available at http://www.lgrecyclingprogram.com/

Mars C., Nafe C., Linnell J, 2016. “the electronics recycling landscape report”. By the Sustainability Consortium ASU & National Center for Electronics recycling. [online document]. [Accessed: 10.11.2017] Available at https://www.sustainabilityconsortium.org/wp-content/uploads/2017/03/TSC_Electronics_Recycling_Landscape_Report-1.pdf

Martin Lokanc, Roderick Eggert, & Michael Redlinger, 2015, The availability of indium: the present, medium term and long term, [online document]. [Accessed: 11.12.2017] Available at https://www.nrel.gov/docs/fy16osti/62409.pdf

Matharu A.S., 2012. Sustainability in LCD Manufacturing, Recycling and Reuse. In: Chen J., Cranton W., Fihn M. (eds) Handbook of Visual Display Technology. Springer, Berlin, Heidelberg, ISBN: 978-3-540-79567-4. DOI: https://doi.org/10.1007/978-3-540-79567-4_166

Measuring screen size, 2001. [online document]. [accessed: 13.12.2017]. Available at http://www.necdisplay.com/Documents/WhitePapers/Measuring_Screen_Size.pdf

Minerals yearbook, 2015. [online document]. [Accessed: 11.12.2017] available at https://minerals.usgs.gov/minerals/pubs/commodity/indium/myb1-2015-indiu.pdf

Minerals commodity summaries 2018. [online document]. [accessed: 18.06.2018] available at: https://minerals.usgs.gov/minerals/pubs/commodity/indium/mcs-2018-indiu.pdf

Periodic-table – indium, [webpage]. [Accessed 10.12.2017] available at http://www.rsc.org/periodic-table/element/49/indium

Press release [web page]. [accessed: 11.12.2017] available at https://technology.ihs.com/431878/us-tv-market-set-for-second-consecutive-year-of-decline-in-2013

Po-Hsun Chen, Ting-Chang Chang, Kuan-Chang Chang, Tsung-Ming Tsai, Chih-Hung Pan, Chih-Cheng Shih, Cheng-Hsien Wu, Chih-Cheng Yang, Wen-Chung Chen, Jiun-Chiu Lin, Ming-Hui Wang, Hao-Xuan Zheng, Min-Chen Chen, Simon M. Sze, 2017. Effects of plasma treatment time on surface characteristics of indium-tin-oxide film for resistive switching storage applications, In Applied Surface Science, Vol 414, pp 224-229. https://doi.org/10.1016/j.apsusc.2017.04.060.

Rocchetti L, Amato A, Fonti V, Ubaldini S, De Michelis I, Kopacek B, Vegliò F, Beolchini F., 2015. Cross-current leaching of indium from end-of-life LCD panels, In Waste Management. 42:180-187. doi: 10.1016/j.wasman.2015.04.035.

Salhofer S., Spitzbart M., Maurer K., 2011, “Recycling of LCD screens in Europe - state of the art and challenges”. In: Hesselbach J., Herrmann C. (eds) Glocalized Solutions for Sustainability in Manufacturing. Springer, Berlin, Heidelberg.

Sami Virolainen, Don Ibana, Erkki Paatero, 2011. Recovery of indium from indium tin oxide by solvent extraction, In Hydrometallurgy, Vol 107, Issues 1–2. pp 56-61, https://doi.org/10.1016/j.hydromet.2011.01.005.

Savolainen Jaakko., 2017. Indium FPD paneelissa (002). [personal communication].

Setis-MIS, 2016. Material information systems – indium. [web page]. [Accessed 10.12.2017] Available at https://setis.ec.europa.eu/mis/material/indium

Shuai Wang, Yaqun He, Tao Zhang, Guangwen Zhang, 2017, "Recovery of valuable components from waste LCD panel through a dry physical method", Waste Management, Vol.64, pp 255-262, https://doi.org/10.1016/j.wasman.2017.03.038.

Silveira A.V. M, Fuchs M. S, Pinheiro D. K, Tanabe E. H, Bertuol D.A., 2015. Recovery of indium from LCD screens of discarded cell phones, In Waste Management. Vol:45 Pages :34-42. https://doi.org/10.1016/j.wasman.2015.04.007

Souada, M., Louage, C., Doisy, J., Ludivine Meunier, Benderrag, A., Ouddane, B., Bellayer, S., Nuns, N., Traisnel, M., Maschke, U., 2018. Extraction of indium-tin oxide from end-of-life LCD panels using ultrasound assisted acid leaching, Ultrasonics Sonochemistry, Volume 40, Part A, Pages 929-936, https://doi.org/10.1016/j.ultsonch.2017.08.043
Strategic-metals, 2017 (webpage) available at http://www.kitco.com/strategic-metals/ accessed: 28.12.2017

Swain, B., Mishra, C., Hong, H. S., Sung-Soo Cho, S., "Beneficiation and recovery of indium from liquid-crystal-display glass by hydrometallurgy", In Waste Management, Volume 57, 2016, Pages 207-214, https://doi.org/10.1016/j.wasman.2016.02.019.

Thin film products, 2017. "thin film products technical data", [online document]. [accessed: 10.01.2018] available at: http://www.thinfilmproducts.umicore.com/Products/TechnicalData/show_datenblatt_ito.pdf

Virolainen, Sami and Paatero, Erkki and Ibana, Don C. 2011. Recovery of indium from LCD screens, in F. Valenzuela and B. Moyer (ed), 19th International Solvent Extraction Conference ISEC 2011, Oct 3-7, 2011. Santiago, Chile: Gecamin.

Wang, H.Y., 2009. A study of the effects of LCD glass sand on the properties of concrete, Waste Management 29, 335–341. https://doi.org/10.1016/j.wasman.2008.03.005.

Yunxia He, En Ma, Zhenming Xu, 2014. Recycling indium from waste liquid crystal display panel by vacuum carbon-reduction, In Journal of Hazardous Materials, Volume 268, Pages 185-190, https://doi.org/10.1016/j.jhazmat.2014.01.011.

Zhang, L., Wu, B., Chen, Y., Xu, Z., 2017. Treatment of liquid crystals and recycling indium for stripping product gained by mechanical stripping process from waste liquid crystal display panels, In Journal of Cleaner Production, Volume 162, 2017, Pages 1472-1481, https://doi.org/10.1016/j.jclepro.2017.06.159.

**Estimation of the mass of ITO for N units of LCD# and the mass of glass residue.**

Mass (g) = density (g/cm$^3$) * volume (cm$^3$) * N

= density (g/cm$^3$) * Area (cm$^2$) * thickness (cm) * N * 2 (CF & TFT layer)

Estimated mass of glass substrate residue.

| Item | LCD1 | LCD2 | LCD3 | LCD4 | LCD5 |
|---|---|---|---|---|---|
| Area (cm$^2$) | 489.5 | 740.25 | 1300.0 | 1228.5 | 1503.5 |
| Mass of ITO (g) | 104.85 | 79.28 | 139.23 | 131.57 | 597.35 |
| Est. mass of residue (kg) | 200.9 | 291.7 | - | 484.7 | 589.4 |

Number of LCD, N = 1000.

**Mass of ITO for 1000 LCD screens**

Density of ITO 7.14 g/cm$^3$

Minimum ITO layer thickness = 150 nm = 0.000015 cm

Mass of ITO (g) =7.14 *489.5 0.000015* 1000*2 = 104.8 g

Estimated mass of the material residue (substrate + polarizer) to be processed for 1000 units of LCD.

Assuming mass of material removed is equal to mass of ITO.

Mass of material residue (kg) = [Mass * 1000 LCD#] – [~ mass of material removed (g)].

APPENDIX II

**Experiment Tables**

Experiment 1. Abrasive brushing process with replication

| # | Grit, X1 | Time/LCD, X2 | No. LCD | Yield, Y1 (g) | Glass (kg) |
|---|---|---|---|---|---|
| LCD 1 | P60 | ~ | 1 | 0 | 0.201 |
| LCD1 | P80 | 240* | 25 | 2.32 | 5.025 |
| LCD2 | P100 | 37 | 18 | 5.66 | 5.256 |
| LCD5 | P100 | 140 | 15 | 8.68 | 8.850 |

* First experiment with hand grinder (4 minutes) per LCD. *

Experiment 2. Heat treatment and abrasive brushing process without replication

| # | Grit size | Time *Seconds*. | Temperature ºC | No. | Yield (g) | Weight of substrate (kg) |
|---|---|---|---|---|---|---|
| LCD1 | P60 | - | 300 | 1 | 0 | 0.201 |
| LCD1 | P80 | - | 300 | 1 | 0 | 0.201 |
| LCD1 | P100 | 240 | 600 | 12 | 2.59 | 2.010 |
| LCD1 | P100 | 240 | 300 | 15 | 3.12 | 3.015 |

The number of experiments was reduced to reflect only the effective combination of parameters.